On the Evolutionary Origin of the Vertebrate Visual System: Insights from the Comparative Researches on the Visual Development of the Lamprey and Amphioxus

A Dissertation Submitted to

the Graduate School of Life and Environmental Sciences,

the University of Tsukuba

in Partial Fulfillment of the Requirements

for the Degree of Doctor of Philosophy of Science

(Doctoral Program in Biological Sciences)

Daichi G. SUZUKI

Contents

Abstract

Vision, especially image-forming vision, provides animals crucial information from environments. In vertebrates, the image-forming vision is evolved independently from those of the crustaceans or cephalopods. To establish the image-forming vision, several visual system components need to be functionally integrated. For example, a camera-type eye forms a image of environmental objects, the optic nerve project to the visual center to send the visual information, the visual center integrates the information with other information and sends motor outputs, and extra-ocular muscles move the eyeball to change the visual field. A key animal to solve this issue is the lamprey, because it shows unique "dual visual development"; in the "primary" phase, the lamprey has only ocellus-like eyes, and in the "secondary" phase, the eyes develops into well-focused mature camera eyes.

Firstly, I analyzed the expression pattern of *Eph* genes in the lamprey. In the results, *EphB* and *EphC* show expression gradients in the "secondary" phase, similar to the gnathostomes. On the other hand, in the "primary" phase, these genes did not show expression gradients, but showed unique pattern. These results indicate that the gnathostomes-type image-forming vision is established in the "secondary" phase and the "primary" phase represents unique state.

Secondly, I focused on the neuroarchitecture of the "primary" visual system in the lamprey. By the neurotrace experiment and the expression pattern analysis on *Pax6*, it is clarified that the "primary" visual center locates in the prosencephalic region. Also, immunohistochemistry experiments and the expression pattern analysis on *Pax6* in amphioxus showed that the visual center of the amphioxus also locates in the prosencephalic region. These results indicate the evolutionary similarity of the visual center between the "primary" phase of the lamprey and

amphioxus.

Finally, I investigated the developmental mechanisms of the extra-ocular muscles (EOMs). The expression analyses revealed that mesodermal patterning and genetic cascade of EOMs are conserved in lampreys, compared to the gnathostomes. However, I found a notable in the expression of muscle differentiation between mesodermal specification phase and determination/differentiation phase, that may cooperate the functional change of the vision in the "dual visual development".

Based on these findings, I discuss the evolutionary origin of the vertebrate visual system. The "dual visual system" of the lampreys seems to represent "recapitulation" from a protochordate-like ancestor to a gnathostome-like vertebrate ancestor, and the vertebrate image-forming vision and the visual system for it evolved *de novo* in the vertebrate lineage.

1. General Introduction

Vision, especially image-forming vision, provides animals crucial information from environments. Based on the visual information, a predator can detect the location of the food and a prey can recognize their enemy.

Parker (2003) argued that the evolution of the image-forming vision caused “Cambrian explosion”, the explosive diversification of animal forms. When a group of the predator evolved it, the animals of the group could ecologically success because they could find much food. On the other hand, each group of their prey evolved its own countermeasure under higher selective pressure. One countermeasure of a prey was to evolve the image-forming vision itself, find its enemy by it, and escape as soon as possible.

Vertebrates are one of the animal groups that evolved the image-forming vision, independently from other groups that evolved the image forming vision; arthropods and cephalopods. Resent findings of a fossil record of the earliest vertebrate *Metaspriggina* suggests that it could possess image-forming vision by its camera-type eye, but was a filter-feeder and used the image-forming vision for the escape behavior (Conway Morris & Caron 2014). And the image-forming vision enabled some groups of the vertebrates to evolve a novel body plan and to change successfully their lifestyle as predators, such as conodonts and gnathostomes (Lacalli 2001).

Since Darwin (1859), a long time issue is how the image-forming vision evolved. To establish the image-forming vision, many visual system components need to be functionally integrated, for example, a camera-type eye, a visual center and the optic nerve projection to it, and extra-ocular muscles for moving the eyeball. Whether there was any evolutionary precursor of the

components for image-forming vision or those evolved *de novo*?

A key animal to solve this issue is the lamprey because it shows unique "dual visual development" described below. And I also study a basal chordate amphioxus, which has only the directional vision, for comparison.

Here, I focus on three components of the visual system; the expression pattern of the *Eph* genes and the development of the topographical retinotectal optic nerve projection (Chapter 2), the "primary" visual center (Chapter 3), and extra-ocular muscles (Chapter 4). And finally (Chapter 5), I discuss the evolution of the vertebrate image-forming vision showing that it evolved *de novo* and the "dual visual development" of the lamprey may represent "recapitulation" from a protochordate-like ancestor to a gnathostome-like vertebrate ancestor.

2. Expression patterns of *Eph* genes in the "dual visual development" of the lamprey and their significance in the evolution of vision in vertebrates

2.1 Abstract

The vertebrate image-forming vision evolved independently from that of other animals and is regarded as a key innovation for enhancing predatory ability and ecological success. This type of vision is achieved with paired camera eyes and topographic projection of the optic nerve. Topographic projection is established by an orthogonal gradient of axon guidance molecules, such as Ephs. To explore the evolution of image-forming vision in vertebrates, lampreys, which belong to the basal lineage of vertebrates, are key animals because they show unique "dual visual development." In the embryonic and pre-ammocoete larval stage (the "primary" phase), photoreceptive "ocellus-like" eyes develop, but there is no retinotectal optic nerve projection. In the late ammocoete larval stage (the "secondary" phase), the eyes grow and form into camera eyes, and retinotectal projection is newly formed. After metamorphosis, this retinotectal projection in adult lampreys is topographic, similar to that of gnathostomes. In this study, I explored the involvement of *Ephs* in lamprey "dual visual development" and establishment of the image-form vision. I found that gnathostome-like orthogonal gradient expression was present in the retina during the "secondary" phase; i.e., *EphB* showed a gradient of expression along the dorsoventral axis, while *EphC* was expressed along the anteroposterior axis. However, no orthogonal gradient expression was observed during the "primary" phase. These results suggest that the "secondary" phase of the lamprey "dual visual development" represents a gnathostomes-like derivative state, and "primary"

phase represents a primitive or lamprey-specific state.

2.2 Introduction

The majority of gnathostomes, the main group of vertebrates, achieve image-forming vision with paired camera eyes and topographic projection of the optic nerve from the retina into the mesencephalic tectum. This topography is established by the orthogonal gradient of axon guidance molecules, such as Ephs, and their ligands, the ephrins (Triplett and Feldheim 2012).

To understand the evolutionary history of the vertebrate visual system and the intermediate stages, lampreys, which belong to an ancestral group of vertebrates (cyclostomes), are key animals because they show unique "dual visual development" (Fig. 2.1).

During the embryonic and pre-ammocoete larval stage (the "primary" phase), only a simple photoreceptive "ocellus-like" eye is formed (Meléndez-Ferro et al. 2002; Villar-Cerviño et al. 2006; Villar-Cheda et al. 2008). The eye of the larval lamprey is under thick and nontransparent skin and has only an immature lens, suggesting that it is not an image-forming eye (Kleerekoper 1972). In addition, the retina of this ocellus-like eye lacks mature amacrine and horizontal cells, but contains photoreceptor, ganglion, and bipolar cells (Villar-Cerviño et al. 2006). Therefore, the ocellus-like eyes are thought to function as nondirectional or broadly directional photoreceptive organs (Villar- Cerviño et al. 2006).

On the other hand, the "secondary" phase corresponds to stages from late ammocoete larvae to adult. During the growth of larvae, the peripheral retinal cells proliferate actively until the metamorphic stage (Villar-Cheda et al. 2008), but most cells remain neuroblastic (de Miguel et al. 1989; Villar-Cerviño et al. 2006). During metamorphosis, these neuroblasts differentiate into photoreceptor, amacrine, and horizontal cells, and the lamprey eye becomes a "truly functional,"

"camera-type eye" in adults (Villar-Cerviño et al. 2006; Villar-Cheda et al. 2008). This camera eye of adult lampreys can process well-focused color vision (Gustafsson et al. 2008).

Furthermore, "dual visual development" is also observed as the development of the optic nerve projection (Fig. 2.1). During the "primary" phase, the optic nerve projects not to the mesencephalic tectum but to the prosencephalic pretectum (described in Chapter 3 in detail). The retinotectal projection develops in older, larger larvae just prior to metamorphosis (de Miguel et al. 1990). Similar to gnathostomes, the retinotectal projection of adult lampreys occurs in a topographic manner (Jones et al. 2009).

In this chapter, I explored the involvement of *Ephs* in lamprey "dual visual development" and establishment of the image-form vision. I first examined whether *Ephs* are involved in the secondary phase to build topographic projections based on their gradient expression. I also examined *Eph* expression during the primary phase to determine whether I can observe any intermediate commitment of *Ephs* during development of the visual system.

2.3 Materials and Methods

Animals

I used *Lethenteron camtschaticum* specimens for embryos and pre-ammocoete larvae. Adult lampreys were collected in the Shiribeshi-Toshibetsu River, Hokkaido, Japan. Mature eggs were squeezed from females and fertilized *in vitro* with sperm. The eggs of some of the females were anesthetized in ethyl 3-aminobenzoate methanesulfonate (MS-222). Embryos were cultured at 16°C. Developmental stages were determined according to Tahara (1988).

Since ammocoete larvae were not readily available for *L. camtschaticum*, I used *Lethenteron* sp. N, the cryptic species of *L. reissneri* (Yamazaki and Goto 1998; Yamazaki et al. 2006), for late stage ammocoete larvae. Ammocoete larvae were collected in the Kamo River, upper Shougawa River, Toyama, Japan, in September.

Isolation of cDNA clones of *Eph* genes

Eph lamprey homologs were isolated by polymerase chain reaction (PCR) using *L. camtschaticum* stage 24–26 embryo cDNA as template. Primers for PCR were designed based on the *Eph* gene sequences of *L. reissneri* (*LrEphB*: AB025542, *LrEphC*: AB025543), which were previously cloned (Suga et al. 1999). The following primers were used: LcEphB-F: 5'-GAGATGGCGGTCGCCATCAAGACGCTAAA-3', LcEphB-R: 5'-TTCTTCTGGTGTCCAGCCAGGGTAACTCC-3', LcEphC-F: 5'-AAGACTCTGAAGGCCGGGTACAGCGAGAA-3',LcEphC-R: 5'-TGCAGGTCTTCCGGTGTCATCTGTGCGAC-3'.

The amino acid sequences of the isolated clones were almost identical to *LrEphB* and *LrEphC*, respectively, and therefore were named *LcEphB* and *LcEphC* (*Lethenteron camtschaticum EphB* and *EphC*; Acc. Nos: AB697185 and AB710343, respectively).

Phylogenetic analysis

The sequences were aligned using MAFFT (Katoh and Toh 2008) and trimmed using trimAL (gap threshold of 50%; Capella-Gutiérrez et al., 2009). Maximum likelihood (ML) trees were inferred using RAxML 7.2.7 and the best-fitting amino acid substitution model, as determined using the RAxML amino acid substitution model selection Perl script (Stamatakis 2006; Stamatakis et al., 2008). Confidence values of the branches were calculated by 1,000 times bootstrappings.

Whole-mount and sectioning for *in situ* hybridization

Whole-mount *in situ* hybridization was performed according to Ogasawara et al. (2000) with minor modifications. Cryosectioning was performed on specimens embedded in Optimal Cutting Temperature (O.C.T.) compound using a CM3050 III (Leica). After washing out the compounds, *in situ* hybridization for cryosectioned materials was performed following the protocol for whole-mount *in situ* hybridization, except that Tween 20 detergent was not used in any step and proteinase treatment was omitted before hybridization. Densitometric scans were performed using ImageJ software. As the retinas were not straight on the sectioned image, densitometry was performed after gray-scale conversion and after splitting the retina into four regions using a computational graphics editor (Photoshop CS6).

2.4 Results

Eph genes in lampreys

Previously, two lamprey *Eph* genes were isolated by Suga et al. (1999), and one was annotated as an orthologue of *EphB*, because it showed a clear affinity to gnathostome *EphB*. The orthology of the second gene was not clear, because it did not show obvious affinity with *EphA* and thus was designated as *EphC*.

In a search of the *Petromyzon marinus* genome (see also Smith et al. 2013), I retrieved eight gene models. However, these gene models should be used with caution, because the lamprey genome is degenerated somatically (Smith et al. 2009, 2012). Thus, this does not necessarily indicate that *Petromyzon* possesses eight *Eph* genes. Phylogenetic analysis showed that three *Eph* genes showed affinities to *EphC*, two to Hagfish *EphA*, and three to cyclostome *EphB* (Fig. 2.2). Among those related to *EphA*, two gene models shared a highly conserved region (approximately 600 bp), including a 100% matching region (200 bp). This region also displayed the same exon structure. Thus, it remains possible that they represent alleles of a single gene. Similarly, three gene models of *EphC* shared three highly conserved regions (approximately 330 bp, 180 bp, and 500 bp, respectively), with the same exon-intron structure. Thus, they may represent alleles or products of alternative splicing or products of genome rearrangement during early embryogenesis (Smith et al. 2009, 2012). Among the *EphB* gene models, two (*PmEphB1* and *PmEphB2*) contain partial sequences with no overlap. Thus, they may originate from a single gene.

Although Suga et al. (1999) annotated Hagfish *EphA* as cognates of gnathostome *EphAs*, the orthology among cyclostome *EphA*, *EphC* and gnathostome *EphAs* remains unclear (Fig. 2.2). It

should be noted that common expression patterns were observed between lamprey *EphC* and gnathostomes *EphAs*, specifically in rhombomeres 3 and 5 (r3 and r5, respectively), suggestive of their evolutionary affinity (Murakami et al. 2004, 2005).

From the transcripts of embryos (stages 25 and 26) and ammocoete larvae (10 cm long), I isolated two *Eph* genes (*EphB* and *EphC)* from *L. camtschaticum*. However, *EphA* transcripts could not be isolated from either stage, suggesting that *EphA* genes were not expressed, or that its expression was low during the stages examined. Thus, I analyzed the expression patterns of *EphB* and *EphC*.

Expression patterns of Eph genes in late ammocoete larvae: the "secondary" phase

In gnathostomes, *EphB* genes show a gradient of expression along the dorsoventral axis with higher expression ventrally in the retina. However, *EphB* does not show an obvious gradient in the mediolateral axis of the tectum (Triplett and Feldheim 2012). *EphA* genes also showed gradient expression, but along the anteroposterior axis with higher levels in the temporal/posterior regions of the retina and in the anterior of the tectum (Triplett and Feldheim 2012).

I examined the expression of *Eph* genes in late ammocoete larvae of approximately 90–130 mm long. At this size, larvae are in the "secondary" phase when the retinotectal optic projection is established. de Miguel et al. (1990) reported that ammocoete larvae longer than 70–80 mm already show retinotectal projection in *Petromyzon marinus* and *Lampetra fluviatilis*.

In the retina of late ammocoete larvae, *EphB* expression was detected in a gradient manner along the dorsoventral axis with higher expression ventrally (Fig. 2.3A), and confirmed it by

densitometric analysis (Fig. 2.4A). On the other hand, I did not detect reproducible gradient patterns along the anteroposterior axis (Fig. 2.3C, 2.4C). I also detected gradient expression of *EphC*, but along the anteroposterior axis with higher expression posteriorly (Fig. 2.3D, 2.4D). However, I did not observe gradient expression along the dorsoventral axis for *EphC* (Fig. 2.3B, 2.4B).

The tectum of lampreys can be divided into the superficial and deeper layers. The optic nerve axons terminate in this superficial layer (Kosareva 1980). Based on expression analysis, both *EphB* and *EphC* showed wide and strong expression in the inner layer of the brain. However, expression in the superficial layer was restricted to the tectum and was not observed in the surrounding brain region (Fig. 2.5, A–D). These expression patterns suggested that Ephs functions as axon guidance molecules. However, my observations did not reveal any expression gradients in the tectum, possibly because of technical limitations in detecting subtle differences in expression levels in sectioned materials.

Expression patterns of *Eph* genes in embryos and pre-ammocoete larvae: the "primary" phase

My analyses in the "secondary phase" revealed an orthogonal gradient of *Ephs*, at least in the retina. Based on these results, I next explored whether a similar pattern was observed during the "primary" phase, when the optic nerve does not project to the mesencephalic tectum but prosencephalic pretectum.

The expression of *EphB* was observed as early as stage 24 in the presumptive diencephalic–rhombencephalic brain, as well as in the upper and lower lips (Fig. 2.6A). The

expression levels in the brain increased at stage 25, especially in the anterodorsal thalamus (Fig. 2.6B). At stage 26, *EphB* expression was detected widely in the brain throughout the diencephalon (thalamus, pineal organ, pretectum, and diencephalic tegmentum), mesencephalon, and rhombencephalon (Fig. 2.6C), but no gradient expression was observed in the tectum or pretectum, the presumptive target for the "primary" optic nerve at this stage (white broken line). In addition, no signal was observed in the eyeball (eb) (Fig. 2.6D). After stage 27 (Fig. 2.6E), *EphB* expression decreased, but was still detected in the anterodorsal thalamus, mesencephalon, and rhombencephalon, as well as in the upper and lower lips and branchial arches.

The expression of *EphC* was detected slightly earlier than *EphB* from stage 23 in the forebrain (fb), r3 and r5, and the trigeminal ganglion (gV; Fig. 2.7A). At stage 24, expression in the forebrain was restricted to the dorsalmost telencephalon, dorsalmost thalamus, and ventral diencephalic tegmentum (tg). It was also expressed in the facial ganglion (gVII) and weakly in rhombomere 6 (r6), as well as the upper and lower lips, somites (sm), and branchial arches (ba; Fig. 7B, B'). At stage 25, expression in the dorsal telencephalon and the anterodorsal thalamus increased. In addition, expression was detected in the eyeball (Fig. 2.7C). During this stage, *EphC* expression was still observed in the rhombomeres (r3 and r5), as reported previously (Murakami et al. 2004). At stage 26, I detected *EphC* expression in the optic stalk, eyeball, and the otic vesicle (otv). Note that in the eyeball, the expression was stronger in the marginal zone (Fig. 2.7D, E). Expression was also detected in the pretectum, which contained the presumptive "primary" optic nerve (Fig. 2.7D', white broken line), but no gradient was observed and instead was present in a uniform manner. The expression of *EphC* clearly decreased after stage 27 (Fig. 2.7F, G).

2.5 Discussion

Establishment of image-forming vision in lampreys

Topography of the retinotectal projection is formed by the orthogonal gradient of axon guidance molecules such as Ephs and ephrins, which forms the basis for image-forming vision in gnathostomes (Triplett and Feldheim 2012).

I found that during the "secondary" phase of lamprey dual visual development, the expression patterns of *Eph* genes showed a gnathostome-like orthogonal gradient in the retina. These gradient patterns were similar to those in gnathostomes; *EphB* showed a gradient of expression along the dorsoventral axis with higher expression ventrally. In addition, *EphC* showed a gradient of expression along the anteroposterior axis with higher expression posteriorly, which was similar to the pattern of gnathostome *EphA*. These results indicate that the topography of the "secondary" phase optic nerve in lampreys is formed by an axon guidance system similar to that of gnathostomes. However, the expression gradients of these genes in the tectum remains unclear, possibly due to technical difficulties in detecting fine quantitative differences in expression levels in sectioned materials. Alternatively, the *Eph* gradient in the retina and *ephrin* gradient in the tectum may be sufficient for the development of the lamprey topographic visual system, although it was difficult to detect the expression of *ephrin* genes due to their short transcript lengths. In addition, I could not isolate any *EphA* transcripts in embryos or ammocoete larvae, indicating that *EphA* genes are expressed at low levels during these stages. However, the common expression patterns between Lamprey *EphC* and gnathostomes *EphAs*, not only in rhombomeres 3 and 5 but also in the gradient manner in retina observed in this study, suggests that they are evolutionary favored compared with

cyclostome *EphAs*.

Despite these issues, the clear gradients of *Eph* gene expression in the retina were consistent with previous observations that the retinotectal optic nerve projection forms during the late larval stage just prior to metamorphosis (de Miguel et al. 1990) and that the retinotectal optic nerve projection in adults is topographic (Jones et al. 2009). Therefore, my results support the hypothesis that the "secondary" optic nerve topography may be mediated by the orthogonal gradient of axon guidance molecules, such as Ephs.

Eph expression in the "primary" phase

My results showed that the expression patterns of *Eph* genes differed during the "primary" phase from those in gnathostomes or during the "secondary" phase of the lamprey. *EphB* expression was not detected in the eyeball. Although both *EphB* and *EphC* expression was detected in the target brain regions of the "primary" optic nerve, the expression was observed widely in the diencephalon and not confined to the specific target region. Furthermore, in the tectum, *EphB* expression did not show gradient expression but instead was observed in a uniform manner. *EphC* was not expressed in the tectum. Thus, neither *EphB* nor *EphC* show gnathostome-like orthogonal gradients in the eyeball, the "primary" visual center or the tectum. These results suggest that the "primary" phase of the lamprey represents evolutionarily primitive state. However, strong expression was observed for *EphC* in the margin of the eyeball of stage 26 larvae (Fig. 4D, E), which may suggest that lamprey *EphC* is involved in the development of the eyeball in a lamprey-specific manner. To examine whether "primary" phase represents primitive or lamprey-specific state, I next analyze "primary"

visual center of the lamprey in the next chapter.

3. A comparative examination of neural circuit and brain patterning between the lamprey and amphioxus reveals the evolutionary origin of the vertebrate visual center

3.1 Abstract

Evolutionary changes in the neural circuits, particularly the visual center, were central for the acquisition of image-forming vision. However, the evolutionary steps, from protochordates to jaw-less primitive vertebrates and then to jawed vertebrates, remain largely unknown. To bridge this gap, I present the detailed development of retinofugal projections in the lamprey, the neuroarchitecture in amphioxus, and the brain patterning in these animals. Both the lateral eye in larval lamprey and the frontal eye in amphioxus project to a light-detecting visual center in the caudal prosencephalic region marked by *Pax6*, which possibly represents the ancestral state of the chordate visual system. My results indicate that the visual system of the larval lamprey represents an evolutionarily primitive state, forming a link from protochordates to vertebrates and providing a new perspective of brain evolution based on developmental mechanisms and neural functions.

3.2 Introduction

As discussed in Chapter 2, "primary" phase in the lamprey "dual visual development" represents unique state, which may be primitive or lamprey-specific. To validate these two possibilities, I focus on the evolution of the visual center. de Miguel et al. (1990) showed that the "primary" optic nerve do not projects to the mecencephalic tectum, but the retino-tectal projection develops in older, larger larvae just prior to metamorphosis. However, the early development of the optic nerve and its projection pattern remain unknown.

Basal chordates amphioxus, on the other hand, have an ocellus-like "frontal eye", but this appears to function only in photoreception and not in image-forming vision. Though amphioxus has multiple photoreceptors, not only the frontal eye but also Hesse ocelli, Joseph cells and lamella body and this indicates that multiple photoreceptors are probably appeared in chordate ancestors, it is considered homologous to the vertebrate paired eyes due to its topology, *Pax6* expression and photoreceptor type (Lacalli 2004). Recent molecular analysis gave further support for homology through the molecular fingerprinting of *Rx*, *Gi* and *c-opsin* in photoreceptor cells and *Mitf* and *Pax2/5/8* in pigment cells (Vopalensky et al. 2012). Lacalli (1996) found the visual center by tracing innervation through electron microscopy and named it "tectum" as a homologous region to the vertebrate mesencephalon. However, the mesencephalon-specific marker gene *Dmbx* is not expressed in the nerve chord of amphioxus, suggesting that amphioxus lacks a mesencephalic region (Takahashi and Holland 2004). Therefore, there is some disagreement on amphioxus neuroarchitecture and brain patterning, making the evolution of vision obscure.

Here I performed comparative examinations on the development of retinofugal projections

in the lamprey, the neuroarchitecture in amphioxus, and the brain patterning in these animals. And based on the results, propose an evolutionary scenario for the visual system in the chordate lineage.

3.3 Materials and Methods

Animals

Adult lampreys (*Lethenteron camtschaticum*) were collected from the Shiribeshi-Toshibetsu River, Hokkaido, Japan. Mature eggs were expelled from females and fertilized *in vitro* by sperm. Adults were anesthetized in ethyl 3-aminobenzoate methanesulfonate (MS-222). Embryos were cultured at 16°C. Developmental stages were determined as described by Tahara (1988).

Collection of larvae of *Branchiostoma japonicum* was done as described by Yasui et al. (1998) and of *B. lanceolatum* as described by Fuentes et al. (2007)

Medaka (*Oryzias latipes*) eggs were incubated at 28°C and then used for neurolabeling experiments.

Whole-mount immunostaining

Whole-mount immunostaining of lampreys (*L. camtschaticum*) with anti-acetylated tubulin monoclonal antibody (Sigma, T6793, RRID: AB477585) was performed according to Kuratani et al. (1997) with some minor modifications. Fixed embryos stored in methanol were washed in TBST containing 5% dimethylsulfoxide (TSTd). The embryos were then blocked with 5% nonfat dry milk in TSTd (TSTM). They were incubated with the primary antibody (diluted 1:1,000 in TSTM) for 2-4 days at room temperature (RT). After washing with TSTd, samples were incubated with secondary antibody (horseradish peroxidase (HRP)-conjugated antibody (Sigma, A2554, RRID: AB258008)) or fluorescence antibody (Invitrogen, Alexa fluor 555, A21424, RRID: AB10566287) diluted 1:200 in TSTM. After a final wash in TSTd, embryos treated with HRP-conjugated antibody

were incubated with the peroxidase substrate in TBST for 1 hour, reacted in TBST with the same concentration of DAB with 0.01% hydrogen peroxide, and examined through an optical microscope. The embryos treated with fluorescent secondary antibody were dehydrated and clarified in a 1:2 mixture of benzyl alcohol and benzyl benzoate (BABB) and then examined using a confocal laser microscope (LSM 510, Zeiss).

Whole-mount immunostaining of amphioxus with anti-acetylated tubulin (Sigma, T6793, RRID: AB477585), synaptotagmin (Sigma, S2177, RRID: AB261464), anti-vesicular acetylcholine transporter (VAChT) (Sigma, V5387, RRID: AB_261875) and anti-serotonin (Sigma, S5545, RRID: AB477522) antibodies was performed according to Kaji et al. (2001) with minor modifications. The primary and secondary antibodies were added together for the double immunostaining with anti-synaptotagmin and anti-acetylated tubulin. Stained specimens were examined using a confocal laser microscope (LSM510, Zeiss).

Neurolabeling

To label the neurons, dextran conjugates (tetramethylrhodamine, 3,000 m. w., Invitrogen, D3308; Alexa Fluor 488, 10,000 m. w., Invitrogen, D22910) were injected into the right eyecup or the caudal rhombencephalon of lamprey embryos or larvae (*L. camtschaticum*) and medaka larvae according to the method described by Glover (1995). The one-color triple labeling was performed by the tetramethylrhodamine-dextran conjugates injection to right eyecup, right forebrain surface, and rhombencephalon at the same time. The two-color double labeling was performed by the sequential labeling of Alexa Fluor 488-dextran conjugates to the rhombencephalon and

tetramethylrhodamine-dextran to the right eyecup with 30 minuites interval. The injected embryos were incubated at RT for 30 minutes to allow anterograde labeling of neuronal projections with dextran. Embryos were then washed with distilled water and fixed in 4% PFA/PBS. The fixed specimens were dehydrated and clarified with BABB. Labeled neurons were examined using a confocal laser microscope.

Isolation of cDNA clones of lamprey and amphioxus genes

Pax6 lamprey homologs were isolated as described by Murakami et al. (2001).

Pax6 amphioxus homologs were isolated by PCR using adult *B. japonicum* cDNA as a template. Primers for PCR were designed on the *Pax6* sequences of *B. floridae* (AJ223440), which have been cloned previously (Glardon et al., 1998). These primer sequences are F: 5'-ATTTCCCGCCTTCTGCAGGTCTCGAATGG-3' and R: 5'-GCCATATTGCCGGGTACGGAAAAGCTTGG-3'.

I isolated a cloned sequence that was orthologous to *BfPax6* (100% match by amino acid sequence), and it was submitted and assigned the DDBJ/EMBL/GenBank accession number AB915169.

Whole-mount and section *in situ* hybridization

Whole-mount *in situ* hybridization for lamprey larvae (*L. camtschaticum*) was performed according to Ogasawara et al. (2000) with minor modifications. Whole-mount *in situ* hybridization for amphioxus larvae was performed as described previously (Wada et al. 1999).

Double staining by *in situ* hybridization and anti-acetylated tubulin immunostaining was

performed following serial treatments. After post-fixation by the NBT/BCIP reaction of *in situ* hybridization, the samples were incubated at RT with 0.1 M glycine-HCl (pH 2.0) for 30 minutes to inactivate alkaline phosphatase. The specimens were then post-fixed with 4% PFA/PBS for 1 hour, washed with PBS and immunostained. The embryos were dehydrated and clarified with BABB and then examined using a confocal microscope. The *in situ* hybridization signals were examined by transmitted light microscopy and the immunostaining signal by specific laser microscopy.

3.4 Results

Early development of the lamprey optic nerve

Immunostaining of anti-acetylated tubulin was performed to examine the temporal profile of lamprey optic nerve development (see also Barreiro-Iglesias et al. 2008; Kuratani et al. 1997, 1998). In stage 24 and stage 25 embryos, some neural fibers (for example, fasciculus retroflexus [FR], medial longitudinal fascicle [MLF], supraoptic tract [SOT], tract of the posterior commissure [TPC]. tract of the postoptic commissure [TPOC]) were observed, but there were no optic fibers (Fig. 3.1A, B). The eyecup (asterisk) and optic fibers (arrow) were first identified during late stage 25 (stage 25.5; 14–15 days post-fertilization; Fig. 3.1C). The eyecups are located just on the ventral region of the ophthalmicus profundus ganglion (gV_1), and the optic fibers are coursed anteriorly toward the chiasm (Ch). In stage 26, the eyecup and optic fibers were present, although it was difficult to distinguish them from the inner brain fibers (Fig. 3.1D). In stage 27, the optic nerve was formed of thin fibers, as noted using confocal microscopy (Fig. 3.1E). In stage 28, the relative position of the eyecup was shifted slightly. It was just ventral to gV_1 at stage 27, but between gV_1 and the trigeminal ganglion ($gV_{2,3}$) at stage 28 (Fig. 3.1F). The opticnerve is thicker compared with the previous stage. It is also notable that the dorsal region of the mesencephalon (Mes) has relatively low immunoreactivity to anti-acetylated tubulin, indicating that there are only a few fibers in this region.

Neurolabeling of lamprey optic nerve projections

I next examined the projection target of the optic nerve by rhodamine-dextran conjugate injection

into lamprey embryos and larvae. The reagent was injected into the right eyecup, and the right optic nerve axons were traced anterogradely (Fig. 3.2A). The optic fibers could be labeled in embryos older than stage 25.5 (Fig. 3.2B). This result is consistent with that of the anti-acetylated tubulin immunostaining. As larvae grew, more fibers were labeled (Fig. 3.2C–F). The tract of posterior commissure (TPC) was also observed as an artifact (Fig. 3.2B, C), because some tracer was taken directly by the brain surface. The optic nerve terminated contralaterally in the left dorsal region forebrain at all stages, and this region was rostral to the tectum, which is located just anterior to the midbrain-hindbrain boundary (MHB). Moreover, ipsilateral retinofugal fibers were not observed at any stage.

I triple labeled the optic nerve, the MLF and the TPC to clarify the target position of the optic nerve projection in the brain. The TPC was situated along the dorsocaudal border of the diencephalon, and the nucleus of the MLF in the ventral region of the posterior commissure. The optic nerve projected to the region ventral to the TPC or nucleus of the MLF (Fig. 3.3A). This region corresponds to the ventral part of the pretectum. Furthermore, I performed two-color double labeling of the optic nerve and the MLF (Fig. 3.3B) and found optic nerve axons with varicosity (see inset of Fig. 3.3B) projecting to dendrites of MLF neurons, suggesting that at least a part of the optic fibers directly connects to MLF neurons.

To verify the brain region receiving the optic projection, I compared nerve tract locations with the expression pattern of *Pax6*, a dorsal prosencephalon marker (Murakami et al., 2001). The *Pax6* expression domain covered the TPC and the nucleus of the MLF situated in its ventral region (Fig. 3.3C). This result is highly consistent with a previous observation (Murakami et al. 2001).

Because the region of the optic nerve projection overlapped with the ventral TPC and nucleus of the MLF, the optic nerve likely projects to a *Pax6*-positive prosencephalic region (P1; pretectum) , but not to the mesencephalic region.

For comparison, I examined optic nerve innervation pattern in medaka as a representative species of gnathostomes by two-color double labeling of optic fibers (magenta) and medial longitudinal fascicle (green). (Fig. 3.3D). In medaka 10 dpf (days post fertilization) larvae, most of the optic fibers (ON) projected to the tectum, and any nMLF-projecting fibers (green) could not be observed in this experiment. These results are consistent with the previous research, which studied retinotectal pathfinding in medaka (Yoda et al. 2004).

Brain patterning and visual center in amphioxus larvae

I next examined brain patterning in amphioxus. Vopalensky et al. (2012) showed the homology between the amphioxus frontal eye and the vertebrate lateral eye by molecular fingerprintings. In addition, they showed innervation by the serotonergic neuron from the frontal eye to the tegmental neuropile, which they suggested is comparable to the vertebrate hypothalamus, although no clear evidence was provided for this homology. Thus, I traced the position of the visual center and examined its homology with the vertebrate neuroanatomical domain by comparing gene expression in this developmental stage. I performed immunostaining using several neural system-related proteins to determine the position of the visual center in amphioxus larvae.

In four gill slit (4gs) larvae, I found anti-serotonin (5-HT)-immunopositive cells located just on the ventral side of the frontal eye pigment (Fig. 3.4A). These cells were identified as R2

cells, as described previously (Holland and Holland 1993; Lacalli 1996; Vopalensky et al. 2012). Furthermore, there were anti-VAChT-immunoreactive neurons (Fig. 3.4B) in 4gs larvae. These cholinergic cells are located in the ventral neural nerve chord; thus, they are ventral component (VC) motor neurons (Bone 1960; Lacalli 2001; Lacalli and Kelly 1999; Candiani et al. 2012). Most rostral cells had relatively large cell bodies. Based on position and cell morphology, these large neurons were likely those identified by Lacalli (1996) as giant cells of the primary motor center in the caudal cerebral vesicle. Between these two types of neurons, I found an anti-synaptotagmin (syt) highly-immunoreactive region (Fig. 3.4C1). Topologically, this region is just rostral to the n2 nerve root (rN2, Fig. 3.4C2) and thought to correspond to the 'tectum' (Lacalli 1996) and its ventral neuropile, containing many synaptic connections. These results suggest that this region may process light information and control movements as a visual center (as at least one of the function of this region), receiving input from rostral sensory neurons and sending output to caudal motor neurons (Fig. 3.4E).

I then performed double staining of *Pax6 in situ* hybridization with acetylated-tubulin immunostaining in one-gill slit (1gs) larvae. At this stage, *Pax6* was expressed in the posterior cerebral vesicle (Fig. 3.4D1, see also Glardon et al. 1998). I found that this region coincides topologically with the rostral region of the n2 nerve root (rN2, Fig. 3.4D2). This indicates that the presumptive visual center in amphioxus larvae is located in the *Pax6* positive region, which may be homologous to the vertebrate prosencephalon as discussed below.

3.5 Discussion

The "primary" optic nerve of lampreys

Lampreys show "dual visual development" of the eye and optic nerve. In embryonic or pre-ammocoete larvae (the "primary" phase), the retina has an ocellus-like form (Melendez-Ferro et al. 2002). In this period, a small number of the optic nerve fibers are formed. In late ammocoete larvae (the "secondary" phase), new optic fibers are formed again. After metamorphosis, adult lampreys have well-developed camera eyes. Thus, I can term the optic nerve formed in the embryonic period as the "primary" optic tract and the one in the newly formed in late larvae as the "secondary" optic tract.

My experiments showed that the "primary" optic tract projects into the *Pax6*-positive neural region (Fig. 3.3). By comparing the expression of *Pax6*, *Otx*, *Dlx1/6*, *Pax2/5/8* and neural tracts marked by anti-acetylated tubulin antibodies, Murakami et al. (2001) indicated that the lamprey prosencephalon can also be identified as a *Pax6* and *Otx*-positive region and the mesencephalon as a *Pax6*-negative and *Otx*-positive region. Therefore, I concluded that the lamprey "primary" optic tract projects into the prosencephalic region but not the mesencephalic region. In the embryonic period, there are opsin-immunoreactive photoreceptor cells in the retina, which may process light information at this stage (Melendez-Ferro et al. 2002). As I found no other retinofugal fibers, I surmised that this neural tract is the only pathway transferring light information from the retina in early larvae (see also De Miguel et al. 1990). This retino-pretectal projection remains as a retinofugal pathway in adult lampreys (Jones et al. 2009). It is thought to function in escape swimming in response to sudden visual stimuli and in dorsal light response (Ullén et al. 1993, 1997;

Deliagina and Fagerstedt 2000). Furthermore, retino-pretectal projection is conserved among gnathostomes. For example, the light reflex of the rat pupil is controlled by the contralateral pretectum (Trejo and Cicerone 1984). And the retino-pretectal projection is also found in hagfish (Kusunoki and Amemiya 1983; Wicht and Northcutt 1990) and blind cave fish (Voneida and Sligar 1976), whose retino-tectal projection is mostly degenerate. Although no diencephalic projection was observed in the stage studied in my experiments (Fig. 3.3D), the adult medaka actually has a number of diencephalic visual centers, such as the pretectum (Deguchi et al. 2005). Also in the zebrafish (Burrill and Easter 1994), the presumptive retio-pretectal projection is observed shortly after the retino-tectal projection (52–54 hpf).

Therefore, the retino-pretectal projection is evolutionarily conserved and probably an ancestral feature of vertebrates. There are fibers of the TPC and nucleus of the MLF in the pretectum region (Fig. 3.3). The TPC fibers integrate left-right information, and the MLF fibers send the signal into the spinal cord. This neuroarchitecture may represent the ancestral visual system.

Visual center similarity in lampreys and amphioxus

I showed the input/output architecture in the visual system of the amphioxus frontal eye, and that the presumptive visual center in amphioxus is located in the *Pax6* expression domain (Fig. 3.4). Therefore, this visual center occupies the same prosencephalic region to that of the region receiving the “primary” optic projections in lamprey, though the segmental neural organization in amphioxus is unclear and detailed synaptic connections between row cells of the amphioxus frontal

eye remains to be studied. Both regions are *Pax6*-positive, receiving visual input and sending output to the trunk, suggesting that this region functions as an integrative visual center (see also Fig. 3.5A). Thus, these regions share close morphological/functional similarity. In addition, Lacalli (2002) showed that the overall structure of the anterior cerebral vesicle change little during metamorphosis in amphioxus. This suggests that the visual center does not change during metamorphosis.

Moreover, in the ascidian *Ciona intestinalis*, putative photoreceptor cells project their axon to other neurons in the posterior sensory vesicle (Imai and Meinertzhagen 2007). Some cholinergic neural cell bodies are located in this region (Yoshida et al. 2004), which is *CiPax6*-positive at the mid-tailbud stage (Mazet et al. 2003). Therefore, the visual center of this species is also located in a *Pax6*-positive region.

On the other hand, there are some differences in the visual neuroarchitecture between lampreys and amphioxus. Serotonergic R2 cells in amphioxus are thought to be homologous to the retinal ganglion cells (RGCs) in vertebrates. But there is no 5-HT immunoreactive RGCs in lamprey before metamorphosis (Abalo e al. 2008). There is another 5-HT immuonoreactive cells in the photoreceptor organ in early lampreys, the pineal organ. Although this organ develops from *Pax6*-positive region, the relationship with R2 cells is also unclear. Moreover, the R2 cells projects ipsilateral (Vopalensky et al. 2012), though the retinal projection in early lamprey is contralateral, as is the often case in vertebrates. However, there are other types of neurons corresponding to the vertebrate retinal neurons, R3 and R4 cells, and especially, R4 cells are thought as possible homologues of RGCs (Lacalli 1996). R4 cells are not serotonergic, and have contralateral projections. They locate just caudal to the R2 cells and have backward-projecting axon like R2 cells.

Therefore I do not dismiss a possibility that other cell types such as R4 cells also act as sensory neurons in the amphioxus frontal eye visual system, and RGCs are homologous to some of these cells rather than R2 cells.

Evolution of vision in the chordate lineage

Based on my findings, I propose an evolutionary scenario for the visual system in chordates (Fig. 6A). The common ancestor of chordates had an ocellus-like eye(s), and the visual center was in the *Pax6*-positive region, where directional vision was processed. These characters are also conserved in tunicates. Moreover, they can be traced back to more ancestral lineages, because the serotonergic neurons found in the amphioxus frontal eye are thought to be homologous to the serotonergic apical organ neurons found in larval echinoderms (Lacalli et al. 1994). Larval hemichordates also have these serotonergic neurons in the apical organ (Miyamoto et al. 2010; Nakajima et al. 2004; Nielsen and Hay-Schmidt 2007). Furthermore, recent research (Marlow et al. 2014) revealed that the origin of the apical organ can be traced back to the common ancestor of cnidarians and bilaterians.

In the common ancestor of vertebrates, the *Pax6*-positive (i.e., prosencephalic) visual center remains one of the main visual center as larval lampreys. Larval lampreys also show some other ancestral states, such as the endostyle (Wright et al. 1980) and the absence of arcualia (Potter and Welsch 1992; Richardson et al. 2010). In addition, the mesencephalic retino-tectal projection was a newly formed "secondary" optic tract in the mesencephalic region. This projection developed a topographical arrangement that enabled the ancestor to establish image-forming vision (Jones et al.

2009).

This scenario also inspires an idea that the evolution of image-forming vision is associated with the evolution of the mesencephalon. However, the emergence of the mesencephalon remains enigmatic. Figure 6B shows the gene regulatory network establishing the mesencephalic region in a vertebrate neural tube. Pani et al. (2012) proposed that the IsO organizer is conserved in the acorn worm. However, Holland et al. (2013) noted that the arrangement of IsO-related genes is reversed and that the organizer activity might not be directly related to the effects on A/P patterning. The *Otx*/*Gbx* boundary and *Pax6* expression is present in amphioxus (underlined), suggesting the existence of the IsO and conserved A/P patterning in the amphioxus neural tube. As neither *Pax2/5/8* nor *En1/2* is expressed in the neural tube just anterior to the *Otx*/*Gbx* boundary, in addition to a lack of *Dmbx* expression, the amphioxus appears to lack a mesencephalic region. Rather, the expression profile of the patterning gene in the anterior neural tube is strikingly similar to that of the vertebrate prosencephalon. My observations in this study are consistent with this idea because the amphioxus visual center, located in the posterior cerebral vesicle, is comparable to the prosencephalic "primary" visual center found in larval lampreys.

4. Morphology and development of extra-ocular muscles in the lamprey reveal the ancestral head structure and its developmental mechanism of vertebrates

4.1 Abstract

The ancestral feature of the vertebrate head has always been one of the intriguing issues in comparative morphology and evolutionary biology. One of the peculiar components of the vertebrate head is extra-ocular muscles (EOMs), whose developmental mechanism and evolution still remain enigmatic: the head mesoderm of elasmobranchs is subdivided and epithelialized as three head cavities, the precursor of EOMs, whereas in avians, they develop from mesenchymal head mesoderm. Importantly, in the basal vertebrate lamprey, the head mesoderm does not show overt head cavities or sign of segmental boundaries, and the development of the EOMs has not been well described. Furthermore, the disposition of differentiated EOMs of the lamprey is different from those of all the other vertebrates, in which the anatomical pattern of EOMs is strongly conserved. To understand the evolution and its developmental origins of the vertebrate EOMs, I explored development of the head mesoderm and EOMs of this animal in detail.

I found that the disposition of EOMs of the lamprey differ from those of gnathostomes, even in the earliest period of development, raising a possibility that the ancestral pattern of EOMs was lamprey-like. I also found that three subpopulations of the head mesoderm could be genetically distinguished (the premandibular mesoderm; *Gsc*+/*TbxA*-, mandibular mesoderm; *Gsc*-/*TbxA*-, hyoid mesoderm; *Gsc*-/*TbxA*+), even if there is no morphological segmentation or epithelialization, indicating that developmental mechanisms of EOMs are basically conserved in the entire

vertebrates.

I argue that the tripartite origins of EOMs were already established in the common ancestor of vertebrates. This ancestor had lamprey-type EOMs, and the disposition of the crown gnathostome EOMs is likely to have secondarily been modified in the lineage of gnathostomes.

4.2 Introduction

The morphological nature or the ancestral feature of the vertebrate head has always been one of the intriguing issues in comparative morphology and evolutionary biology. One of the peculiar components of the vertebrate head is extra-ocular muscles (EOM), which control the visual field by moving paired eyes. They are derived from the head mesoderm and their development has attracted a great deal of morphologists' attention in the controversy of ancestral head structure, whether the head mesoderm is segmented or not.

Those who believe the segmentation of the head mesoderm, insisted that the segmentation is typically observed in the shark cranial development (Neal and Rand 1946). In the traditional scheme, the head mesoderm of elasmobranch embryos forms three pairs of head cavities, the premandibular (pmc), mandibular (mc), and hyoid cavities (hc), which later differentiate into six extra-ocular muscles (EOMs) innervated by three cranial nerves; the oculomotor (III), the trochlear (IV), and the abducens nerve (VI) (see also Fig. 1C, Fig. 10). Though these head cavities are often degenerated in other gnathostomes, vestigial head cavities are occasionally found in bony fishes and amniotes (Brachet 1935; Fraser 1915; Wedin 1953; Jacob et al. 1984; Kuratani et al. 2000), implying that possession of these cavities is a shared, derived characteristic of gnathostomes, though it is secondarily diminished in the majority of members.

In avian, the head cavities are degenerated except the premandibular cavity (Adelmann 1926), but presence of pseudosegmental blocks in the head mesoderm, so-called "somitomeres", is detected by using scanning electron microscopy (reviewed by Jacobson 1993). Though the existence of these somitomeres are doubted (reviewed by Kuratani 2003), the EOMs develop from

the part of the head mesoderm (both premandibular and paraxial) located in positions similar to shark head cavities (Couly et al. 1993; Jacob et al. 1984; Noden 1983, 1988; Noden and Francis-West 2006; Wachtler et al. 1984; Wachtler and Jacob 1986).

Classically, the head mesoderm of lampreys was also thought to be segmented along the anteroposterior axis like head cavities in elasmobranch embryos (Koltzoff 1901; Neal 1918; Damas 1944), and EOMs differentiate from three head cavities innervated from respective motor nerves (Koltzoff 1901; Neal 1918). However, Kuratani et al. (1999) reported, by scanning electron microscopy-based observation of Japanese marine lamprey, Lethenteron camtschaticum, that there are no cavities, or sign of segmental boundaries in the head mesoderm, and insisted that the ancestral head mesoderm of the vertebrates is likely to have been unsegmented and uniform (Fig. 1D), raising a question as to how the EOMs develop from this unsegmented, uniform head mesoderm.

In addition, anatomical disposition and the innervation pattern of EOMs are highly conserved among gnathostomes so much so that Neal (1918) once noted that "[t]heir 'evolutionary potential' appears to be approximately zero". However, those of lampreys are far different from that of gnathostomes (Nishi 1938; Shimazaki 1965; Fritzsh et al. 1990; Fig. 1). In gnathostomes, the oculomotor nerve innervates four of the EOMs (medial rectus, mr; superior rectus, sr; inferior rectus, ir; inferior oblique, io), whereas the trochlear and abducens innervate only single EOMs, superior oblique (so) and lateral rectus (lr), respectively. On the other hand, the lamprey oculomotor nerve innervates only three EOMs (anterior rectus, ar; dorsal rectus, dr; anterior oblique, ao), the abducens innervates two (ventral rectus, vr; caudal rectus, cr). Also, the caudal oblique (co) muscles,

which is innervated by the trochlear nerve, attaches to the orbit far more caudally than that of gnathostomes does. Since EOMs have completely degenerated in the other group of cyclostomes hagfishes (Nishi 1938), the lamprey is the key extant animal to estimate ancestral state of the EOMs and its developmental mechanisms in the context of "the head problem".

To understand evolutionary origin of the vertebrate EOMs and to speculate a possible ancestral state of the vertebrate head, I examined the detailed development of the embryonic head mesoderm and EOMs in lampreys. I found that the developmental mapping of EOMs is conserved also in the lamprey since the muscle originated from three distinct domains within the head mesoderm, but their disposition was different already by the differentiation into muscles. This indicates that the developmental patterning of EOMs from the three subdivisions of the head mesoderm was already established in the common ancestor of vertebrates. Based on these findings, I discussed about the ancestral state of the vertebrate head mesoderm and its differentiation.

4.3 Materials and Methods

Animals

Adult lampreys (*Lethenteron camtschaticum*, synonym *L. japonicum*) were collected from the Shiribeshi-Toshibetsu River, Hokkaido, Japan. Adults were anesthetized in ethyl 3-aminobenzoate methanesulfonate (MS-222). Mature eggs were expelled from females and fertilized *in vitro* by sperm. Embryos were cultured at 16°C, fixed by three days in 4% paraformaldehyde in 0.1 M phosphate-buffered saline (PBS) and dehydrated in a graded methanol series, and stored in 100% methanol at −20 °C. Developmental stages were determined as described by Tahara (1988).

As ammocoete larvae were not readily available for *L. camtschaticum*, we used *Lethenteron* sp. N, the cryptic species of *Lethenteron reissneri* (Yamazaki and Goto 1998; Yamazaki et al. 2006), for ammocoete larvae. These larvae were collected in the Kamo River, Upper Shougawa River, Toyama, Japan, in September.

Histological analyses

Lethenteron sp. N were fixed in Bouin's or Serra's fixative, dehydrated, and embedded in paraffin. Sections were cut at a thickness of 6 μm and stained with hematoxylin and eosin, according to a standard technique.

Whole-mount immunofluorescence

Whole-mount immunofluorescence with anti-acetylated tubulin (Sigma, T6793, RRID: AB477585) and anti-CH1 (Hybridoma bank) antibodies was performed according to Kuratani et al. (1997) with

some minor modifications. Fixed embryos stored in methanol were washed in TBST containing 5% dimethylsulfoxide (TSTd). The embryos were then blocked with 5% nonfat dry milk in TSTd (TSTM). They were incubated with the primary antibody (diluted 1:1,000 in TSTM) for 2-4 days at room temperature (RT). After washing with TSTd, samples were incubated with fluorescence secondary antibody (Invitrogen, Alexa fluor 555, A21424, RRID: AB_10566287) diluted 1:200 in TSTM. After a final wash in TSTd, embryos were dehydrated and clarified in a 1:2 mixture of benzyl alcohol and benzyl benzoate (BABB) and then examined using a confocal laser microscope (LSM 510, Zeiss).

Whole-mount and section *in situ* hybridization

RNA probes were synthesized from cDNA clones. *PitxA*, *MrfA* and *MA2* are already isolated (*PitxA*: Uchida et al. 2003; *MrfA*, *MA2*: Kusakabe et al. 2011). A plasmid of *TbxA* is provided by Dr. M. Tanaka (isolated by Onimaru et al. 2011). *Gsc* were isolated from *L. camtschaticum* by RT-PCR from stage 25 specimens using the following primers designed for *Petromyzon* genes (*PmGsc*, HQ248103;) (Cerny et al. 2010). Whole-mount *in situ* hybridization was performed according to Ogasawara et al. (2000) with minor modifications. For section *in situ* hybridization, larval lampreys (*Lethenteron* sp. N) were fixed for three days in 4% paraformaldehyde in 0.1 M phosphate-buffered saline (PBS), dehydrated, and embedded in paraffin. Sections were cut at a thickness of 8 μm. After washing out the paraffin, *in situ* hybridization for cryosectioned materials was performed following the protocol for whole-mount *in situ* hybridization, except that Tween 20 detergent was not used in any step and proteinase treatment was omitted before hybridization.

Cell labeling

Stage 21 embryos were injected with 1mM DiI, DiD DiO solutions (Vybrant Multicolor Cell-labeling kit, Molecular Probes). The embryos were excised from the egg membranes and placed in wells made in a solidified agar in a plastic dish. Injections were performed with a fine glass pipet. The embryos were incubated for 10 days until they reached approximately stage 27 and were fixed in 4% paraformaldehyde in PBS. Observation was performed with fuorescence microscope or confocal microscope (LSM510, Zeiss).

4.4 Results

Development of EOMs and their innervations

In order to see whether the disposition of the lampre EOMs changed during their development from a small leave to an adult, I performed a histological analysis by the hematoxylin-eosin (HE) staining on the extraocular muscles in the small larva (3.5 cm, about a half year old, Fig.4.2A), large larva (10 cm, Fig. 4.2B), metamorphic (Fig. 4.2C), and adult lamprey (Fig. 4.2D). In small larva, EOMs were found as fibrous, discriminable six cell clusters (Fig. 4.2A). From its disposition, each EOM could be identified. In large larva, EOMs become compartmented and much discriminable (Fig. 4.2B). In the metamorphic stage, the external part of the EOMs became thinner and wider (Fig. 4.2C1), suggesting that they attached to eyeball rigidly to move it functionally. These changes seem to represent their unique life style that the lampreys spend about four or five years as ammocoetes larvae, which do not possess image-forming vision (Kleerekoper 1972; Villar-Cerviño et al. 2006, see also Chapter 2 and Chapter 3), and after the metamorphosis, they stick to their prey using well-developed image-forming vision (Gustafsson et al. 2008). Finally in the adult (Fig. 4.2D), I confirmed that there are six EOMs deposited as same as that was observed by gross anatomy (Fig.4.1E). Through all stages examined, the whole disposition of the EOMs was almost same, so, it is likely to be already arranged before metamorphosis. But it is notable that there is a little change with the relationship between the anterior rectus (ar) and anterior oblique (ao). While in the larval period, these muscles are situated side by side in its muscle origins (Fig 4.2B4), they crosses over themselves in adults (Fig. 4.2D4, see also Fig. 4.1E).

Developmental mechanism of EOMs and patterning of head mesoderm

For a further trace back on the developmental origin of the lamprey EOMs, immunfluorescense of anti-CH1 (tropomyosin) antibody was performed to examine early development of larval EOMs in lampreys (Fig.4.3A–C). Either in stage 28 and 30 pro-ammocoete larvae, I did not detect EOM by anti-CH1, and only detect somatic/branchial muscles; supraoclularis (supraoc), subocuralis (suboc), elevator labialis ventralis (elv), velocranialis (vc), and constrictor buccalis (cb) (Fig. 4.3A,B, see also Hardisty and Rovainen 1982).

Thus, I tried to trace developmental origin by using more upstream regulatory genes for EOMs. In the gnathostomes, genetic cascade in the development of EOMs were already reported; muscle-related factors (MRFs) act as determination and differentiation genes, and *Pitx2* acts upstream of MRFs in cranial muscle progenitor cells and *Pitx2* null embryos lack EOMs (Sambasivan et al. 1999). This pattern is also conserved in sharks, where *Pitx2* and *Myf5* (a member of the MRF family) are expressed in developing head mesoderms/cavities (Adachi et al. 2012).

In st. 26 lamprey larvae, though expressions of *MrfA* (a member of the MRF family) or *MA2* (muscle differentiation marker) were not detected (Kusakabe et al. 2011), I detected *Pitx2* expression in the head mesoderm (Fig. 4.4A). On the other hand, in 9 cm ammocoete larvae, *MrfA* and *MA2* were expressed in EOMs, while *Pitx2* expression was almost decreased (Fig. 4.5).

Furthermore, I found that there was distinct genetic patterning between subpopulations of the head mesoderm and this is conserved among vertebrates. *Gsc* is expressed in the prechordal plate in gnathostomes (de Robertis et al. 1994) and premandibular mesoderm is come from it (lampreys: Kuratani et al. 1999; sharks: Adachi and Kuratani 2012). I found that *Gsc* is expressed in

the anterior head mesoderm in st. 26 lamprey (Fig. 4.4B), and this expression corresponded to the premandibular mesoderm (pm) on overlap with the anterior expression of *Pitx*. At the same stage, *TbxA* was expressed in the anterior region of otic vesicle (otv) (Fig. 4.4C). In sharks, corresponding expression is also observed and it is thought as the expression in the hyoid cavity (Adachi et al. 2012), so this expression could also regarded as the expression in the hyoid mesoderm (hm). These results indicates that the head mesoderm of lamprey, which is marked by *PitxA*, is actually subdivided by gene expressions of *Gsc* and *TbxA*; the premandibular mesoderm is *Gsc*+ and *TbxA*-, the mandibular mesoderm is *Gsc*- and *TbxA*- and the hyoid mesoderm is *Gsc*- and *TbxA*+ (Fig. 4.4D).

Developmental lineage of the head mesoderm; from its origin to the differentiated EOMs

By examining expressions of *Pitx*, *Gsc* and *Tbx,* I found that head mesoderm were subdivided into three populations similar to those of gnathostomes that differentiate into EOMs. I thus examined the three populations of lamprey head mesoderm would differentiate to EOMs innervated respective motor nerves like the shark head cavities, by the immunofluorescence of anti-acetylated tubulin. In st. 28, though the head mesoderm was not differentiated to the EOMs yet (Fig. 4.3A), *PitxA* was expressed in the three head mesodermal subpopulations (Fig. 4.6A). In this stage, the innervation nerves of EOMs were already extending their fibers in this stage, and their distribution pattern was corresponded to the each subpopulations of the head mesoderm; the oculomotor nerve (III) to the premandibular mesoderm, the trochlear nerve (IV) to the mandibular mesoderm, and the abducens nerve (VI) to the hyoid mesoderm (Fig. 4.6B, C, see also Fig. 4.8). These fivers were prolonged to

the orbit by 15mm larvae (Fig. 4.6D), and their distribution pattern is maintained in the larval period, when the EOMs were already formed (35mm; Fig. 4.6E, see also Fig. 4.3C). These results indicated that the three populations of the head mesoderm attracted their respective innervation nerves and differentiate to the EOMs with their respective innervation nerves, supporting that the head mesoderm populations differentiate into EOMs.

It is thought that the premandibular head mesoderm is derived from the prechordal plate, and the mandibular and hyloid mesoderm is regionized by the first phalyngeal pouch rostrocaudally (Kuratani et al. 1999). Based on my results (Fig. 4.4), each population is likely to be genetically patterned by *Gsc* and *TbxA*. But there is another possibility that the mesenchyme cells are mixed and re-regionalized by these genes. Thus, I performed cell-labeling experiments to test whether each population of the head mesoderm retain their cohesion from its origin or become mixed. Firstly, only DiO was injected to the prechordal plate region in st. 21 embryos (Fig. 4.7A) and incubated to st. 27. In the st. 27 larvae, DiO signal was observed around eyeball, though eyeball itself was also labeled as an artifact (Fig. 4.7B, C). Subsequently, three-color labeling was performed; DiO was injected to the prechordal plate region, DiI was to the mandibular mesoderm, and DiD was to the hyoid mesoderm (Fig. 4.7D). As a result, almost all larvae (N= 43/48, there was no fluorescent signal observed in the rest 5 samples), these mesodermal population retained their cohesion and do not become mixed (Fig. 4.7E). The positions of these populations also corresponded to the expression patterns of *Gsc* and *TbxA* as described above (Fig. 4.4D, E). These results showed that the three populations of the head mesoderm were specified by the patterning genes such as *Gsc* and *TbxA*, and retained their cohesion.

4.5 Discussion

Developmental mechanism of the EOMs and the head mesoderm

In the present study, in order to infer the evolutionary history of vertebrate EOMs, I traced developmental process of EOMs in lampreys, because the morphological distributions of EOMs were distinct from those of gnathostomes. I found that the overall distribution of the lamprey EOMs are established as early as 32mm larvae (approximately a half year old, Fig. 4.3C). Thus, lampreys and gnathostomes show distinct distribution of EOMs when they are recognized as differentiated muscles (lamprey: Fig. 5C; chick: reviewed in Noden and Francis-West 2006).

In contrast, the genetic cascade concerning the development of head mesoderm is conserved in the lamprey. Furthermore, the expression pattern of *Gsc* and *TbxA* (Fig. 4.4) suggested that three populations of the head mesoderm (the premandibular, mandibular, and hyoid mesoderm) underlie distinct genetic identities and this is conserved among vertebrates. In addition, these populations retained their cohesion and attract their respective innervation nerves (Fig. 4.6, 4.7), like the shark head cavities, even if there is no morphological segmentation in the lamprey (Kuratani et al. 1999).

However, because I did not detect the muscle differentiation marker such as the *MA2* gene or the CH1 antibody at the developmental stage when *Pitx*, *Gbx* and *Tbx* were detected, it was not clear whether the *Pitx* positive head mesoderm indeed differentiate into EOMs in the lampreys. I overcame this issue by examining the innervation of motor neurons to head mesoderm. I presented evidences that, although at this stage mosucle marker was not detected, motor neuron innervation was observed when *Pitx* expression was detected. As the result, the oculomotor nerve (III)

innervated to the premandibular mesoderm, the trochlear nerve (IV) to the mandibular mesoderm, and the abducens nerve (VI) to the hyoid mesoderm (Fig. 4.6B, C, see also Fig. 4.8). This innervation pattern supported that the lamprey EOMs differentiate from the three head mesoderm populations.

Figure 4.8 shows the comparison of EOM development between the lamprey and shark. In both species, primarily the head mesoderm is uniform (Fig. 4.8A, D). But the coherence of each subpopulation is retained and they attract their respective innervation nerve (Fig. 4.8B, E). In this stage, the head mesoderm in the shark is epithelized to the head cavities (Adachi and Kuratani 2012). Finally, EOMs are differentiated from each mesodermal population in respective disposition in each species (Fig. 4.8C, F). This comparison indicates that the developmental mechanisms of EOMs from three populations of the head mesoderm were already established in the common ancestor of vertebrates (Fig. 4.9).

Ancestral state of EOMs, their developmental mechanism and what caused the difference between the lamprey and gnathostomes

The above comparison of development of EOMs between lampreys and gnathostomes indicates that evolutionary modification of EOMs must have occurred during the developmental stage after three head mesoderm populations established, but before muscle differentiation commences (corresponding to the stage between stage 28 and 3.5 cm early larva of lampreys). But it is not clear from this study, which type of EOM distribution is ancestral for the vertebrates. Previous studies on fossil records (Young 1986, 2008; Janvier 1985, 1996) revealed that the disposition of EOMs in

osteoderms and placoderms is more similar to that of lampreys than of the crown gnathostomes (osteichthyans and chondrichthyans). Therefore, the ancestral disposition of EOMs is more likely to be the lamprey-type, and the extant-gnathostome-type disposition likely to represent derived pattern only specific in the crown gnathostomes (Fig. 4.9). The modification might be functionally linked with the postorbital connection between the palatoquadrate and neurocranium, which is a synapomorphy of the crown gnathostomes (Young 1986). As the caudal oblique muscle could interfere the postorbital connection between the palatoquadrate and neurocranium, the position of the caudal oblique muscle might have changed to anterior in the orbit.

The evolutionary of the vertebrate head

My findings indicated that the common ancestors of the vertebrates possessed three populations of the head mesoderm, although clear morphological segmentation may not be visible. These head mesoderm eventually differentiate into EOMs, which are likely to be distributed as in the present-day lampreys. However, it remains enigmatic how these head structure and its developmental mechanism was evolved, or the origin of the vertebrate head. There are two major hypothesis; vertebrate head was newly appeared (the "new head" theory: Gans and Northcutt 1983), or acquired by losing the epithelial segmentation of the most anterior paraxial mesoderm of the amphioxus-like ancestor (Bertrand et al. 2011).

Protochordate amphioxus also possess anterior mesoderm cells which express *Pitx*. In the amphioxus, though *Pitx* genes is expressed in the anterior somite and mesodermal Hatschek's diverticulum (Boorman and Shimeld 2002). Although these *Pitx* positive cells of amphioxus may

possess evolutionary link with the vertebrate EOMs and pituitary, expressions of *Gsc* or *Tbx1* was not observed in these *Pitx* positive cells (Neidert et al. 2000:Mahadevan et al. 2004). Therefore, even if the amphioxus anterior mesoderm cells are evolutionary origin of head mesoderm, they must be in more immature status. Subdivision of the head mesoderm into three populations must have occurred in the common ancestors of the vertebrates. Further characterization of the anterior mesoderm of amphioxus would be required to solve the issue of the origin of the vertebrate head.

5. General Discussion

The vertebrate visual system is a complex system consisted of several components, for example, a camera-type eye, a visual center and the optic nerve projection to it, and extra-ocular muscles for moving the eyeball. It is long time issue is how this complex system evolved, as Darwin (1859) noted,

> *To suppose that the eye, with all its inimitable contrivances for adjusting the focus to different distances, for admitting different amounts of light, and for the correction of spherical and chromatic aberration, could have been formed by natural selection, seems,*
> *I freely confess, absurd in the highest possible degree.*

The evolutionary origin of the photoreceptor cells is also enigmatic. There are two types of the photoreceptor cell in animal; rhabdomeric and ciliary photoreceptrors. The protostomes usually has rhabdomeric photoreceptor, and the deuterostomes uses ciliary photoreceptor. The common ancestor of these two lineages, the urbilateria, seems to have had both type and rhabdomeric cells evolved to other retinal cells (horizontal, amacrine, and retinal ganglion cells) in vertebrate lineage (Arendt 2003).

Vertebrates are one of the animal groups that evolved the image-forming vision, independently from other groups that evolved the image forming vision; arthropods and cephalopods. To clarify the evolutionary origin of the vertebrate visual system, I focused on the visual development in the basal vertebrate lamprey in this study, because the lamprey shows unique "dual visual development"; in the "primary" phase, the lamprey has only ocellus-like eyes, and in the "secondary" phase, the eyes develops into well-focused mature camera eyes.

Firstly, I explored the expression pattern of the *Eph* gene in Chapter 2. The axon guidance molecule *Eph* is required for the development of the topographical retinotectal optic nerve projection in the gnathostomes, showing orthogonal gradient expression in retina and tectum. But in the lamprey's "dual retinal development", the gradient expression was observed only in the "secondary phase"; i.e., *EphB* showed a gradient of expression along the dorsoventral axis, while *EphC* was expressed along the anteroposterior axis. However, no orthogonal gradient expression was observed during the "primary" phase. These results suggest that the "secondary" phase of the lamprey "dual visual development" represents a gnathostomes-like derivative state, and "primary" phase represents a primitive or lamprey-specific state.

Secondary, I investigated detailed development of retinofugal projections in the lamprey, the neuroarchitecture in amphioxus, and the brain patterning in these animals in Chapter 3. Both the lateral eye in larval lamprey and the frontal eye in amphioxus project to a light-detecting visual center in the caudal prosencephalic region marked by *Pax6*, which possibly represents the ancestral state of the chordate visual system. My results indicate that the visual system of the larval ("primary" phase) lamprey represents an evolutionarily primitive state, forming a link from protochordates to vertebrates and providing a new perspective of brain evolution based on developmental mechanisms and neural functions.

And finally, I studied the development of the extra-ocular muscles in lamprey in chapter 4. I found that the disposition of EOMs of the lamprey differ from those of gnathostomes, even in the earliest period of development, raising a possibility that the ancestral pattern of EOMs was lamprey type-like. I also found that three subpopulations of the head mesoderm could be genetically

distinguished (the premandibular mesoderm; *Gsc*+/*TbxA*-, mandibular mesoderm; *Gsc*-/*TbxA*-, hyoid mesoderm; *Gsc*-/*TbxA*+), even if there is no morphological segmentation or epithelialization, indicating that developmental mechanisms of EOMs are basically conserved in the entire vertebrates. In addition, the development of EOMs of the lamprey showed a prolonged process in the larval period and the EOMs seemed to become functional in the metamorphosis, cooperating with the "dual visual development".

Similar to their "dual visual development", lampreys show remarkable transformation during metamorphosis from a protochordate-type character status to a vertebrate-type status. For example, the endostyle (without follicle) in the larval stage transforms into the thyroid gland (with follicle) during metamorphosis (Wright et al. 1980). In addition, no arcualia (vertebral rudiments) are observed in the larval stage, but they appear after metamorphosis (Potter and Welsch 1992; Richardson et al. 2010). From an evolutionary perspective, these transformations may represent "recapitulation" from a protochordate-like ancestor to a gnathostome-like vertebrate ancestor. Youson (2004) proposed that ancestral lampreys were marine and capable of reproduction in a larval-like form. Invasion of iodine-poor fresh water caused evolution of follicle for storage of the iodine that is required for thyroid hormone (TH) synthesis, which is a factor in the evolution of metamorphosis. The "secondary" phase seems to co-evolved *de novo* with the evolution of metamorphosis and this is applicable to "princible of terminal addition" in the typical recapitulation (Gould 1977).

However, the hagfishes, the other group of cyclostomes, are a direct-developer. Thus it remains still enigmatic whether the common ancestor of the vertebrates represented direct-

development like the hagfishes, or indirect-development like the lampreys. It is need to be studied that the conservation of the metamorphosis mechanism in the vertebrates for estimating the metamorphosis is derived from the common ancestor or not.

Acknowledgements

I would like to like to express my sincere thanks to Professor Hiroshi Wada (University of Tsukuba) for his generous support and critical discussion. I am indebted to reviewes, Associate Professor Chikafumi Chiba (University of Tsukuba), Professor Katsuo Furukubo-Tokunaga (University of Tsukuba) and Professor Masanao Honda (University of Tsukuba), for their critical reading of the manuscript. I am grateful to Associate Professor Yasunori Murakami (Ehime University) for his advices and suggestions.

I thank Professor Hector Escriva (Centre national de la recherche scientifique, CNRS), Associate Professor Yuji Yamazaki (Toyama University) and Mr. Tadashige Kishi (Hiyama Fisheries Cooperative) for their cooporation in collecting animals. I also thank the members of the Wada lab. for their discussions and supports.

Research grants from the Japan Society for the Promotion of Science (JSPS) funded this work.

References

Abalo XM, Villar-Cerviño V, Villar-Cheda B, Anadón R, Rodicio MC. 2008. Neurochemical differentiation of horizontal and amacrine cells during transformation of the sea lamprey retina. J Chem Neuroanat 35:225–232.

Adachi N, Kuratani S. 2012. Development of head and trunk mesoderm in the dogfish, *Scyliorhinus torazame*: I. Embryology and morphology of the head cavities and related structures. Evol Dev 14:234–256.

Adachi N, Takechi M, Hirai T, Kuratani S. 2012. Development of the head and trunk mesoderm in the dogfish, *Scyliorhinus torazame*: II. Comparison of gene expression between the head mesoderm and somites with reference to the origin of the vertebrate head. Evol Dev 14:257–276.

Adelmann HB. 1926. The development of the premandibular head cavities and the relations of the anterior end of the notochord in the chick and robin. J Morph Phys 42:371–439.

Arendt D. 2003. Evolution of eyes and photoreceptor cell types. Int J Dev Biol 47:563–571.

Barreiro-Iglesias A, Villar-Cheda B, Abalo XM, Anadón R, Rodicio MC. 2008. The early scaffold of axon tracts in the brain of a primitive vertebrate, the sea lamprey. Brain Res Bull 75:42–52.

Bertrand S, Camasses A, Somorjai I, Belgacem MR, Chabrol O, Escande M-L, Pontarotti P, Escriva H. 2011. Amphioxus FGF signaling predicts the acquisition of vertebrate morphological traits. Proc Natl Acad Sci USA 108:9160–9165.

Bone Q. 1960. The central nervous system in amphioxus. J Comp Neurol 115:27–64.

Boorman CJ, Shimeld SM. 2002. Pitx homeobox genes in *Ciona* and amphioxus show left–right

asymmetry is a conserved chordate character and define the ascidian adenohypophysis. Evol Dev 4:354–365.

Brachet A. 1935. Traité d'Embryologie des Verteébrés. Masson & Cie, Etiteurs, Paris.

Burrill JD, Easter SS Jr. 1994. Development of the retinofugal projections in the embryonic and larval zebrafish (*Brachydanio rerio*). J Comp Neurol 346:583–600.

Candiani S, Moronti L, Ramoino P, Schubert M, Pestarino M. 2012. A neurochemical map of the developing amphioxus nervous system. BMC Neurosci 13:59

Capella-Gutiérrez S, Silla-Martínez JM, Gabaldón T. 2009. trimAl: a tool for automated alignment trimming in large-scale phylogenetic analyses. Bioinformatics 25:1972–1973.

Cerny R, Cattell M, Sauka-Spengler T, Bronner-Fraser M, Yu F, Medeiros DM. 2010. Evidence for the prepattern/cooption model of vertebrate jaw evolution. Proc Natl Acad Sci USA 107:17262–17267.

Couly GF, Coltey PM, Le Douarin NM. 1993. The triple origin of skull in higher vertebrates: a study in quail-chick chimeras. Development 117:409–429.

Damas H. 1944. Recherches sur le développement de *Lampetra fluviatilis* L.—Contribution à l'étude de la cephalogénèse des vertébrés. Arch Biol Paris 55:1–289.

Darwin C. 1859. On the Origin if Species. John Murray, London.

Deguchi T, Suwa H, Yoshimoto M, Kondoh H, Yamamoto N. 2005. Central connection of the optic, oculomotor, trochlear and abducens nerves in medaka, *Oryzias latipes*. Zoolog Sci 22:321–332.

Deliagina TG, Fagerstedt P. 2000. Responses of reticulospinal neurons in intact lamprey to vestibular and visual inputs. J Neurophysiol 83:864–878.

de Miguel E, Rodicio, MC, Anadón R. 1989. Ganglion cells and retinopetal fibers of the larval lamprey retina: an HRP ultrastructual study. Neurosci Lett 106:1–6.

de Miguel E, Rodicio, MC, Anadon R. 1990. Organization of the visual system in larval lampreys: an HRP study. J Comp Neurol 302:529–542.

de Robertis EM, Fainsod A, Gont LK, Steinbeisser H. 1994. The evolution of vertebrate gastrulation. Development:117–124.

Fraser EA. 1915. The head cavities and development of the eye muscles in *Trichosurus vulpecula*, with notes on some other marsupials. Proc Zool Soc 22:299–346.

Fritzsch B, Sonntag R, Dubuc R, Ohta Y, Grillner S. 1990. Organization of the Six Motor Nuclei Innervating the Ocular Muscles in Lamprey. J Comp Neurol 294:491–506.

Gans C, Northcutt RG. 1983 Neural crest and the origin of vertebrates: A new head. Science 220:268–273.

Glardon S, Holland LZ, Gehring WJ, Holland ND. 1998. Isolation and developmental expression of the amphioxus *Pax-6* gene (*AmphiPax-6*): insights into eye and photoreceptor evolution. Development 125:2701–2710.

Glover JC. 1995. Retrograde and anterograde axonal tracing with fluorescent dextran amines in the embryonic nervous system. Neurosci Protoc 30:1–13.

Gould SJ. 1977. Ontogeny and Phylogeny. Belknap Press of Harvard University Press, Cambridge.

Gustafsson OSE, Collin SP, Kröger RHH. 2008. Early evolution of multifocal optics for well-focused colour vision in vertebrates. J Exp Biol 211:1559–1564.

Hardisty MW, Rovainen CM. 1982. Morphological and functional aspects of the muscular system.

In: Hardisty MW, Potter IC, eds. The Biology of Lampreys, volume 4A. Academic Press, London. pp 137–232.

Holland ND, Holland LZ. 1993. Serotonin-containing cells in the nervous system and other tissues during ontogeny of a lancelet, *Branchiostoma floridae*. Acta Zool 74:195–204.

Holland LZ, Carvalho J, Escriva H, Laudet V, Schubert M, Shimeld SM, Yu JK. 2013. Evolution of bilaterian central nervous systems: a single origin? EvoDevo 4:27.

Imai JH, Meinertzhagen IA. 2007. Neurons of the ascidian larval nervous system in *Ciona intestinalis*: I. Central nervous system. J Comp Neurol 334:316–334.

Jacob M, Jacob HJ, Wachtler F, Christ B. 1984. Ontogeny of avian extrinsic ocular muscles. I. A light and electron-microscopic study. Cell Tissue Res 237:549 – 557.

Jacobson AG. 1993. Somitomeres: Mesodermal segments in the head and trunk. In: Hanken J, Hall BK, eds. The Vertebrate Skull. Vol. 1. University Chicago Press, Chicago. pp. 42–76.

Janvier P. 1985. Les Céphalaspides du Spitsberg. Centre National de la Recherche Scientifique, Paris.

Janvier P. 1996. Early Vertebrates. Clarendon Press, Oxford.

Jones MR, Grillner S, Robertson B. 2009. Selective projection patterns from subtypes of retinal ganglion cells to tectum and pretectum: distribution and relation to behavior. J Comp Neurol 517:257–275.

Kaji T, Aizawa S, Uemura M, Yasui K. 2001. Establishment of left-right asymmetric innervation in the lancelet oral region. J Comp Neurol 435:394–405.

Katoh K, Toh H. 2008. Recent developments in the MAFFT multiple sequence alignment program.

Brief Bioinfo 9:286–298.

Kleerekoper H. 1972. The sense organ. In: Hardisty MW, Potter IC, eds. The Biology of Lampreys, vol. 2. Academic Press, London. pp 373–404.

Koltzoff NK. 1901. Entwicklungsgeschichte des Kopfes von *Petromyzon planeri*. Bull Soc Nat Moscou 15:259–289.

Kosareva AA. 1980. Retinal projections in lamprey (*Lampetra fluviatilis*). J Hirnforsch 21:243–256.

Kuratani S. 2003. Evolutionary developmental biology and vertebrate head segmentation: a perspective from developmental constraint. Theor Biosci 122:230–251.

Kuratani S, Horigome N, Hrano S. 1999. Developmental morphology of the head mesoderm and reevaluation of segmental theories of the vertebrate head: evidence from embryos of an agnathan vertebrate, *Lampetra japonica.* Dev Biol 210:381–400.

Kuratani S, Horigome N, Ueki T, Aizawa S, Hirano S. 1998. Stereotyped axonal bundle formation and neuromeric patterns in embryos of a cyclostome, *Lampetra japonica*. J Comp Neurol 391:99–114.

Kuratani S, Nobusada Y, Saito H, Shigetani Y. 2000. Morphological characteristics of the developing cranial nerves and mesodermal head cavities in sturgeon embryos from Early pharyngula to late larval stages. Zool Sci 17:911–933.

Kuratani S, Ueki T, Aizawa S, Hirano S. 1997. Peripheral development of cranial nerves in a cyclostome, *Lampetra japonica*: morphological distribution of nerve branches and the vertebrate body plan. J Comp Neurol 384:483–500.

Kusakabe R, Kuraku S, Kuratani S. 2011. Expression and interaction of muscle-related genes in the

lamprey imply the evolutionary scenario for vertebrate skeletal muscle, in association with the acquisition of the neck and fins. Dev Biol 350:217– 227.

Kusunoki T, Amemiya F. 1983. Retinal projections in the hagfish, *Eptatretus burgeri*. Brain Res 262:295–298.

Lacalli TC. 1996. Frontal eye circuitry, rostral sensory pathways and brain organization in amphioxus larvae: evidence from 3D reconstructions. Phil Trans R Soc Lond B 351:243–263.

Lacalli TC. 2001. New perspectives on the evolution of protochordate sonsory and locomotory systems, and the origin of bains and heads. Phil Trans R Soc Lond B 356:1565–1572.

Lacalli TC. 2002. Sensory pathways in amphioxus larvae I. Constituent fibres of the rostral and anterodorsal nerves, their targets and evolutionary significance. Acta Zool 83:149–166.

Lacalli TC. 2004. Sensory systems in amphioxus: a window on the ancestral chordate condition. Brain Behav Evol 64:148–162.

Lacalli TC, Holland ND, West JE. 1994. Landmarks in the anterior central nervous system of amphioxus larvae. Phil Trans R Soc Lond B 344:165–185.

Lacalli TC, Kelly SJ. 1999. Somatic motoneurones in amphioxus larvae: cell types, cell position and innervation patterns. Acta Zool 80:113–124.

Mahadevan NR, Horton AC, Gibson-Brown JJ. 2004. Developmental expression of the amphioxus *Tbx1/10* gene illuminates the evolution of vertebrate branchial arches and sclerotome. Dev Genes Evol 214:559– 566.

Marlow H, Tosches MA, Tomer R, Steinmets P, Lauri A, Larsson T, Arendt D. 2014. Larval body patterning and apical organs are conserved in animal evolution. BMC Biol 12:7.

Mazet F, Hutt J, Millard J, Shimeld S. 2003. Pax gene expression in the developingcentral nervous system of *Ciona intestinalis*. Gene Expression Patterns 3:743–745.

Meléndez-Ferro M, Villar-Cheda B, Abalo XM, Perez-Costas E, Rodriguez-Munoz R., Degrip WJ, Yanez J, Rodicio MC, Anadón R. 2002. Early development of the retina and pineal complex in the sea lamprey: comparative immunocytochemical study. J Comp Neurol 442:250–265.

Miyamoto N, Nakajima Y, Wada H, Saito Y. 2010. Development of the nervous system in the acorn worm *Balanoglossus simodensis*: insights into nervous system evolution. Evol Dev 12:416–424.

Murakami Y, Ogasawara M, Sugahara F, Hirano S, Satoh N, Kuratani S. 2001. Identification and expression of the lamprey *Pax6* gene: evolutionary origin of the segmented brain of vertebrates. Development 128:3521–3531.

Murakami Y, Pasqualetti M, Tako Y, Hirano S, Rijili FM, Kuratani S. 2004. Segmental development of reticulospinal and branchiomotor neurons in lamprey: insights into the evolution of the vertebrate hindbrain. Development 131:983–995.

Murakami Y, Uchida K, Rijlia F. M, Kuratani S. 2005. Evolution of the brain developmental plan: Insights from agnathans. Dev Biol 280:249–259.

Nakajima Y, Humphreys T, Kaneko H, Tagawa K. 2004. Development and neural organization of the tornaria larva of the Hawaiian hemichordate, *Ptychodera flava*. Zool Sci 21:69–78.

Neal HV. 1918. The history of the eye muscles. J Morphol 30:433–453.

Neal HV, Rand HW. 1946. Comparative Anatomy. Blakiston, Philadelphia.

Neidert AH, Panopoulou G, Langeland JA. 2000. Amphioxus *goosecoid* and the evolution of the

head organizer and prechordal plate. Evol Dev 2:303–310.

Nielsen C, Hay-Schmidt A. 2007. Development of the Enteropneust *Ptychodera flava*: ciliary bands and nervous system. J Morphol 570:551–570.

Nishi S. 1938. B. Augenmuskulatur. In: Bolk L, Göppert E, Kallius E, Lubosch W, eds. Handbuch der vergreichenden Anatomie der Wirbeltiere, Band 5. Urban und Schwarzenberg, Wien. pp 453–466.

Noden DM. 1983 The embryonic origins of avian cephalic and cervical muscles and associated connective tissues. Am J Anat 168: 257–276.

Noden DM. 1988. Interactions and fates of avian craniofacial mesenchyme. Development: 103 121–140.

Noden DM, Francis-West P. 2006. The Differentiation and Morphogenesis of Craniofacial Muscles. Dev Dyn 235:1194–1218.

Ogasawara M, Shigetani Y, Hirano S, Satoh N, Kuratani S. 2000. *Pax1/Pax9*-Related genes in an agnathan vertebrate, *Lampetra japonica*: expression pattern of *LjPax9* implies sequential evolutionary events toward the gnathostome body plan. Dev Biol 223:399–410.

Onimaru K, Shoguchi E, Kuratani S, Tanaka M. 2011. Development and evolution of the lateral plate mesoderm: Comparative analysis of amphioxus and lamprey with implications for the acquisition of paired fins. Dev Biol 359:124–136.

Pani AM, Mullarkey EE, Aronowicz J, Assimacopoulos S, Grove EA, Lowe CJ. 2012. Ancient deuterostome origins of vertebrate brain signaling centres. Nature 483:289–294.

Parker, A. 2003. In the Blink of an Eye: How Vision Sparked the Big Bang of Evolution. Perseus

Pub, Cambridge.

Potter IC, Welsch U. 1992. Arrangement, histochemistry and fine structure of the connective tissue architecture of lampreys. J Zool 225:1–30.

Richardson MK, Admiraal J, Wright GM. 2010. Developmental anatomy of lampreys. Biol Rev 85:1–33.

Sambasivan R, Gayraud-Morel B, Dumas G, Cimper C, Paisant S, Kelly RG, Tajbakhsh S. 1999. Distinct regulatory cascades govern extraocular and pharyngeal arch muscle progenitor cell fate. Dev Cell 16:810–821.

Shimazaki S. 1965. Kontribuo al la Kompara Anatomio de Okulmuskoloj če Ciklostomoj kaj Fîsoj. Acta Anat Nip 40:354–367.

Stamatakis A. 2006. RAxML-VI-HPC: Maximum Likelihood-based Phylogenetic Analyses with Thousands of Taxa and Mixed Models. Bioinformatics 22:2688–2690.

Stamatakis A, Hoover P, Rougemont J. 2008. A Rapid Bootstrap Algorithm for the RAxML Web-Servers. Syst Biol 57:758–771.

Suga H, Hoshiyama D, Kuraku S, Katoh K, Kubokawa K, Miyata T. 1999. Protein tyrosine kinase cDNAs from amphioxus, hagfish, and lamprey: isoform duplications around the divergence of cyclostomes and gnathostomes. J Mol Evol 49:601–608.

Smith JJ, Antonacci F, Eichler EE, Amemiya CT. 2009. Programmed loss of millions of base pairs from a vertebrate genome. Proc Natl Acad Sci USA 106:11212–11217.

Smith JJ, Baker C, Eichler EE. Amemiya CT. 2012. Genetic consequences of programmed genome

rearrangement. Curr Biol 22:1524–1529.

Smith JJ, Kuraku S, Holt C, Sauka-Spengler T, Jiang N, Campbell MS, Yandell MD, et al. 2013. Sequencing of the sea lamprey (*Petromyzon marinus*) genome provides insights into vertebrate evolution. Nat Genet 45:415–421.

Tahara Y. 1988. Normal stages of development in the lamprey, *Lampetra reissneri* (Dybowski). Zool Sci 5:109–118.

Takahashi T, Holland PWH. 2004. Amphioxus and ascidian Dmbx homeobox genes give clues to the vertebrate origins of midbrain development. Development 131:3285–3294.

Trejo LJ, Cicerone CM. 1984. Cells in the pretectal ovaly nucleus are in the pathway for the firect light reflex of the pupil in the rat. Brain Res 300:49–62.

Triplett JW, Feldheim DA. 2012. Eph and ephrin signaling in the formation of topographic maps. Semin. Cell Dev Biol 23:7–15.

Uchida K, Murakami Y, Kuraku S, Hirano S, Kuratani S. 2003. Development of the adenohypophysis in the lamprey: evolution of epigenetic patterning programs in organogenesis. J Exp Zool B 300:32–47.

Ullén F, Orlovsky GN, Deliagina TG, Grillner S. 1993. Role of dermal photoreceptors and lateral eyes in initiation and orientation of locomotion in lamprey. Behav Brain Res 54:107–110.

Ullén F, Deliagina TG, Orlovsky GN, Grillner S. 1997. Visual pathways for postural control and negative phototaxis in lamprey. J Neurophysiol 78:960–976.

Villar-Cerviño V, Abalo XM, Villar-Cheda B, Meléndez-Ferro M, Pérez-Costas E, Holstein GR, Martinelli GP, Rodicio MC, Anadón R. 2006. Presence of glutamate, glycine, and γ-

aminobutyric acid in the retina of the larval sea lamprey : Comparative immunohistochemical study of classical neurotransmitters in larval and postmetamorphic retinas. J Comp Neurol 499:810–827.

Villar-Cheda B, Abalo XM, Villar-Cerviño V, Barreiro-Iglesias A, Anadón R, Rodicio MC. 2008. Late proliferation and photoreceptor differentiation in the transforming lamprey retina. Brain Res 1201:60–67.

Vopalensky P, Pergner J, Liegertova M, Benito-Gutierrez E, Arendt D, Kozmik Z. 2012. Molecular analysis of the amphioxus frontal eye unravels the evolutionary origin of the retina and pigment cells of the vertebrate eye. Proc Natl Acad Sci USA 109:15383–15388.

Voneida TJ, Sligar CM. 1976. A comparative neuroanatomic study of retinal projections in two fishes: *Astyanax hubbsi* (the blind cave fish), and *Astyanax mexicanus.* J Neurosci 165:89–105.

Wada H, Garcia-Fernàndez J, Holland PWH. 1999. Colinear and segmental expression of amphioxus Hox genes. Dev Biol 213:131–141.

Wachtler F, Jacob M. 1986. Origin and development of the cranial skeletal muscles. Biblthca Anat 29:24–46.

Wachtler F, Jacob HJ, Jacob M, Christ B. 1984. The extrinsic ocular muscles in birds are derived from the prechordal plate. Naturwissenschaften 71:379–380.

Wedin B. 1953. The origin and development of the extrinsic ocular muscles in the alligator. J Morph 92:303–336

Wicht H, Northcutt RG. 1990. Retinofugal and retinopetal projections in the Pacific hagfish, *Eptatretus stouti* (Myxinoidea). Brain Behav Evol 36:315–328.

Wright GM, Filisa MF, Youson JH. 1980. Immunocytochemical localization of thyroglobulin in the transforming endostyle of anadromous sea lampreys, *Petromyzon marinus* L., during metamorphosis. Gen Comp Endocr 42:187–194.

Yamazaki Y, Goto A. 1998. Genetic structure and differentiation of four *Lethenteron* taxa from the Far East, detected from allozyme analysis. Env Biol Fish 52:149–161.

Yamazaki Y, Yokoyama R, Nishida M, Goto A. 2006. Taxonomy and molecular phylogeny of *Lethenteron* lampreys in eastern Eurasia. J Fish Biol 68:251–269.

Yasui K, Tabata S, Ueki T, Uemura M, Zhang SC. 1998. Early development of the peripheral nervous system in a lancelet species. J Comp Neurol 393:415–425.

Yoda H, Hirose Y, Yasuoka A, Sasado T, Morinaga C, Deguchi T, Henrich T, Iwanami N, Watanabe T, Osakada M, Kunimatsu S, Wittbrodt J, Suwa H, Niwa K, Okamoto Y, Yamanaka T, Kondoh H, Furutani-Seiki M. 2004. Mutations affecting retinotectal axonal pathfinding in Medaka, *Oryzias latipes*. Mech Dev 121:725–728.

Yoshida R, Sakurai D, Horie T, Kawakami I, Tsuda M, Kusakabe T. 2004. Identification of neuron-specific promoters in *Ciona intestinalis*. Genesis 39:130–140.

Young GC. 1986. The relationships of placoderm fishes. Zool J Linn Soc 88:1–57.

Young GC. 2008. Number and arrangement of extraocular muscles in primitive gnathostomes: evidence from extinct placoderm fishes. Biol Lett 4:110–114.

Youson JH. 2004. The impact of environmental and hormonal cues on the evolution of fish metamorphosis. In: Hall BK, Pearson RD, Muller GB, eds. Environment, Development, and Evoleution: Toward a Systhesis. Massachusetts Institute of Technology Press, Cambridge. pp

239–278.

Figures

Fig. 2.1. Schematic diagram of "dual visual development," adapted from de Miguel et al. (1990), Jones et al. (2009), Meléndez-Ferro et al. (2002) and Villar-Cheda et al. (2008). By the pre-ammocoete larval stage, the eyeball (eb) and optic stalk (os) are formed by evagination of the brain. The lens (ls) is flattened and the retina (R) is small. The "primary" optic nerve (ON^1) projects into the pretectum, and not to the tectum (tc). According to larval growth, the eyes grow again by proliferation of the peripheral (lateral) retina. During the late ammocoete stage, the newly developed "secondary" optic nerve (ON^2) projects to the tectum. In the lateral retina, neuroblastic cells (NbCs) remain undifferentiated, except retinal ganglion cells and their optic nerve fibers. In the central retina (CR), photoreceptor cells are already differentiated. After metamorphosis, in the adult, the retinotectal optic nerve projection is topographic, and NbCs are differentiated. Abbreviations: eb, eyeball; ls, lens; NbCs, neuroblastic cells; ON^1, "primary" optic nerve; ON^2, "secondary" optic nerve; os, optic stalk; R, retina; tc, tectum.

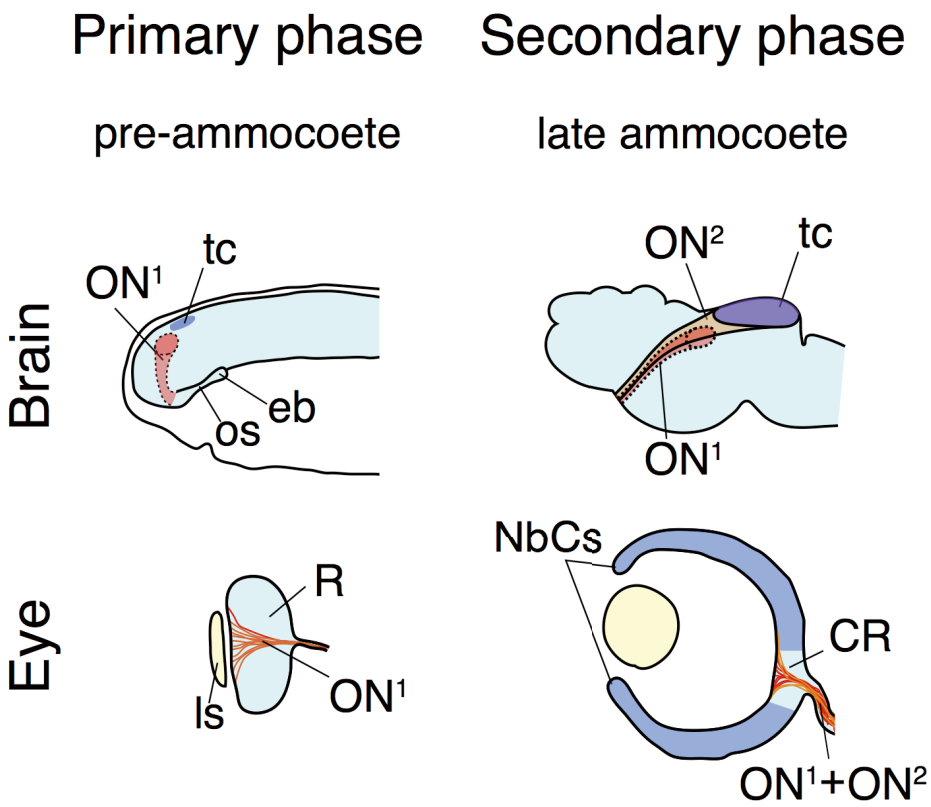
Primary phase
Secondary phase
pre-ammocoete
late ammocoete
Brain
Eye
ON1
tc
eb
os
ON2
tc
ON1
R
ON1
ls
NbCs
CR
ON1+ON2

Fig. 2.2. Molecular phylogenetic tree for Eph genes. The tree was constructed using the ML method. The numbers at the nodes represent bootstrap values. Lc: *L. camtschaticum*, Lr: *L. reissneri*, Pm:*P. marinus*.

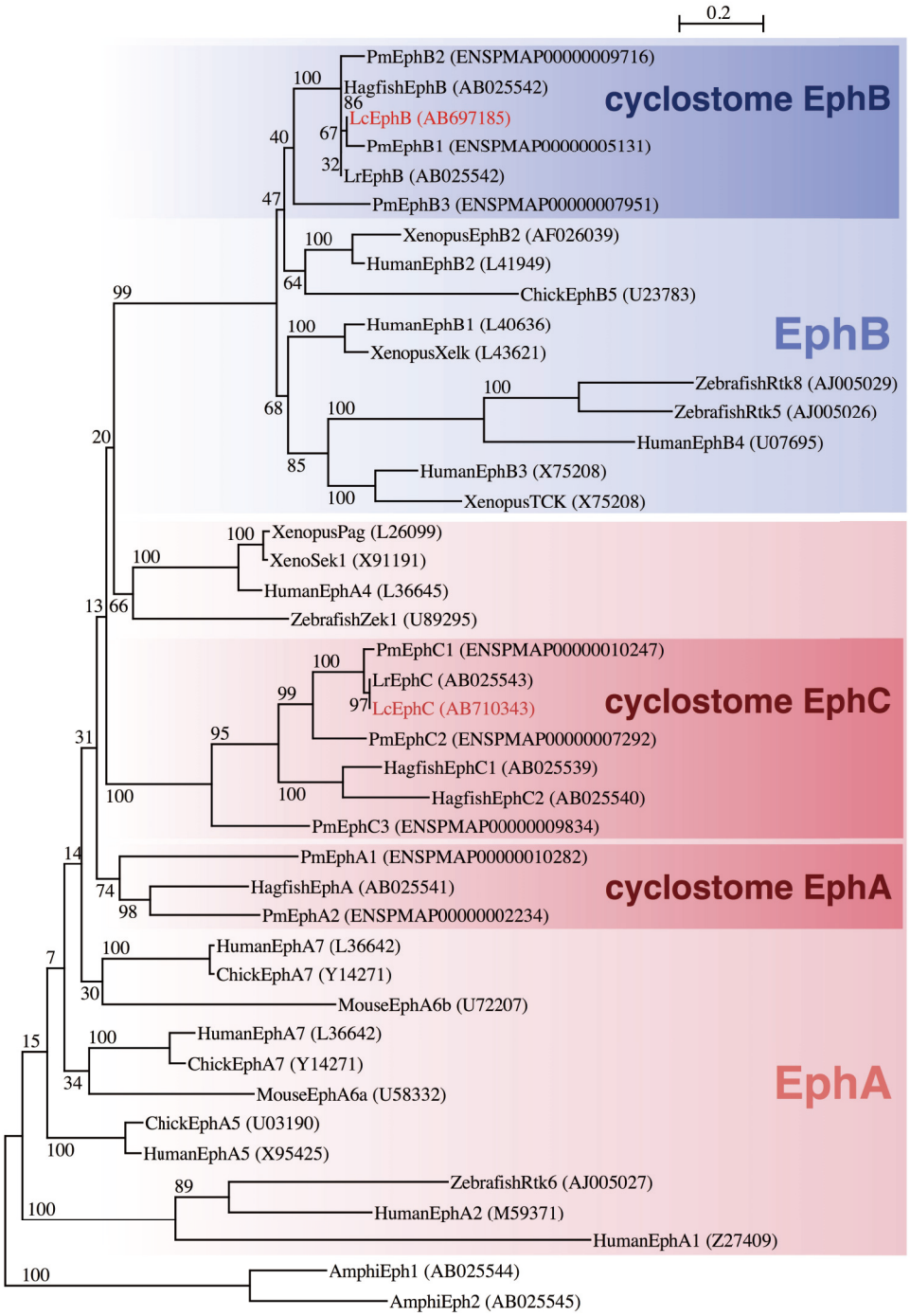
0.2
PmEphB2 (ENSPMAP00000009716)
HagfishEphB (AB025542)
LcEphB (AB697185)
PmEphB1 (ENSPMAP00000005131)
LrEphB (AB025542)
PmEphB3 (ENSPMAP00000007951)
cyclostome EphB
XenopusEphB2 (AF026039)
HumanEphB2 (L41949)
ChickEphB5 (U23783)
HumanEphB1 (L40636)
XenopusXelk (L43621)
ZebrafishRtk8 (AJ005029)
ZebrafishRtk5 (AJ005026)
HumanEphB4 (U07695)
HumanEphB3 (X75208)
XenopusTCK (X75208)
EphB
XenopusPag (L26099)
XenoSek1 (X91191)
HumanEphA4 (L36645)
ZebrafishZek1 (U89295)
PmEphC1 (ENSPMAP00000010247)
LrEphC (AB025543)
LcEphC (AB710343)
PmEphC2 (ENSPMAP00000007292)
HagfishEphC1 (AB025539)
HagfishEphC2 (AB025540)
PmEphC3 (ENSPMAP00000009834)
cyclostome EphC
PmEphA1 (ENSPMAP00000010282)
HagfishEphA (AB025541)
PmEphA2 (ENSPMAP00000002234)
cyclostome EphA
HumanEphA7 (L36642)
ChickEphA7 (Y14271)
MouseEphA6b (U72207)
HumanEphA7 (L36642)
ChickEphA7 (Y14271)
MouseEphA6a (U58332)
ChickEphA5 (U03190)
HumanEphA5 (X95425)
ZebrafishRtk6 (AJ005027)
HumanEphA2 (M59371)
HumanEphA1 (Z27409)
EphA
AmphiEph1 (AB025544)
AmphiEph2 (AB025545)

Fig. 2.3. Sections of *in situ* hybridization in late ammocoete larvae of lampreys (*L.* sp. N) in the retina. **A, B:** In transverse sections of the retina, a gradient of *EphB* expression was observed along the dorsoventral axis with strong expression ventrally (arrow). In contrast, *EphC* showed uniform expression. **C, D:** In horizontal sections, while *EphB* showed uniform expression, a gradient of *EphC* expression was observed along the anteroposterior axis with stronger expression posteriorly (arrow). Abbreviations: di, diencephalon; tc, tectum; tg tegmentum. Scale bar: 200 μm.

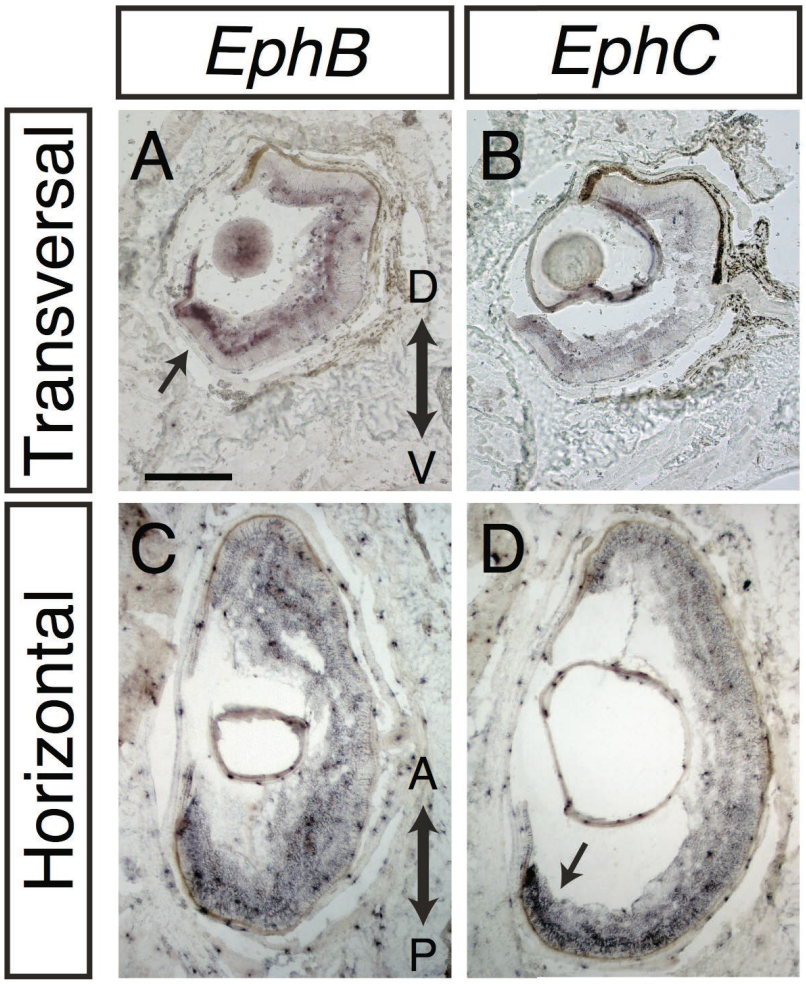
EphB
EphC
Transversal
Horizontal
A
B
C
D
D
V
A
P

Fig. 2.4. Densitometric scan on the *EphB* and *EphC* expression patterns in the retina of the late ammocoete larvae shown in Fig. 3. The scan is performed after gray-scale conversion, cutting region by region along the retina (boxes in **A1**, **B1**, **C1** and **D1**) and linearization. The results of the scan are shown in A2, B2, C2 and D2, respectively. **A, B:** Transverse sections. **A:** *EphB*. **B:** *EphC*. **C, D:** Horizontal sections. **C:** *EphB*. **D:** *EphC*.

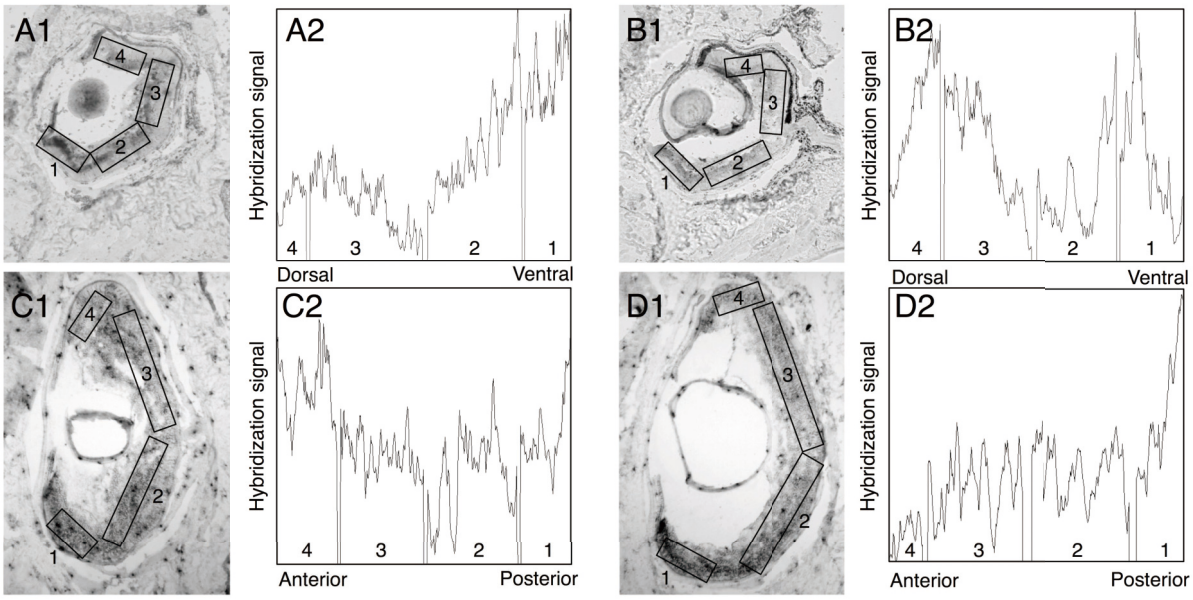
A1
4
3
2
1
A2
Hybridization signal
4
3
2
1
Dorsal
Ventral
B1
4
3
2
1
B2
Hybridization signal
4
3
2
1
Dorsal
Ventral
C1
4
3
2
1
C2
Hybridization signal
4
3
2
1
Anterior
Posterior
D1
4
3
2
1
D2
Hybridization signal
4
3
2
1
Anterior
Posterior

Fig. 2.5. Sections of *in situ* hybridization in late ammocoete larvae of lampreys (*L* sp. N) in the tectum. **A, B:** In transverse sections of the tectum, both *EphB* and *EphC* showed uniform expression in the inner layer of the tectum and tegmentum. In the superficial layer, the expression was restricted to the tectum, but no clear gradient of expression was observed. **C, D:** In horizontal sections, *EphB* and *EphC* expression was observed in the inner layer of the tectum and diencephalon. However, expression in the superficial layer was restricted to the tectum. Broken lines indicate the border of the tectum in the superficial layer and asterisks indicate the border of the tectum in the deep layer. Abbreviations: di, diencephalon; tc, tectum; tg tegmentum. Scale bar: 200 μm.

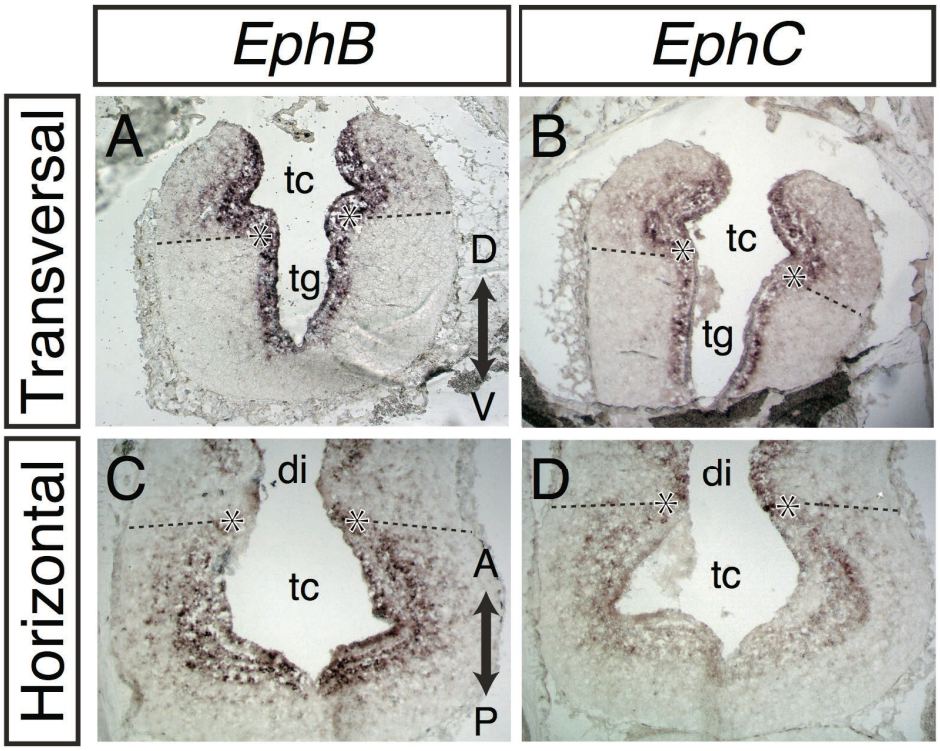
EphB
EphC
Transversal
Horizontal
A
B
C
D
tc
tg
di
D
V
A
P

Fig. 2.6. Whole-mount *in situ* hybridization of *EphB* in lamprey embryos and pre-ammocoete larvae (*L. camtschaticum*). White broken lines indicate the dorsocaudal thalamus and pretectum region, which is the presumptive target region of "primary" optic nerves. At stages **A:** 24, **B:** 25, and **C:** 26. **D:** In a transverse section at the level of the eyeball (eb) at stage 26 and **E:** stage 27. Abbreviations: ba, branchial arches; eb, eyeball; es, endostyle; ll, lower lip; mes, mesencephalon; MHB, mid–hindbrain boundary; po, pineal organ; rho, rhombencephalon; th, thalamus. Scale bar: 200 μm.

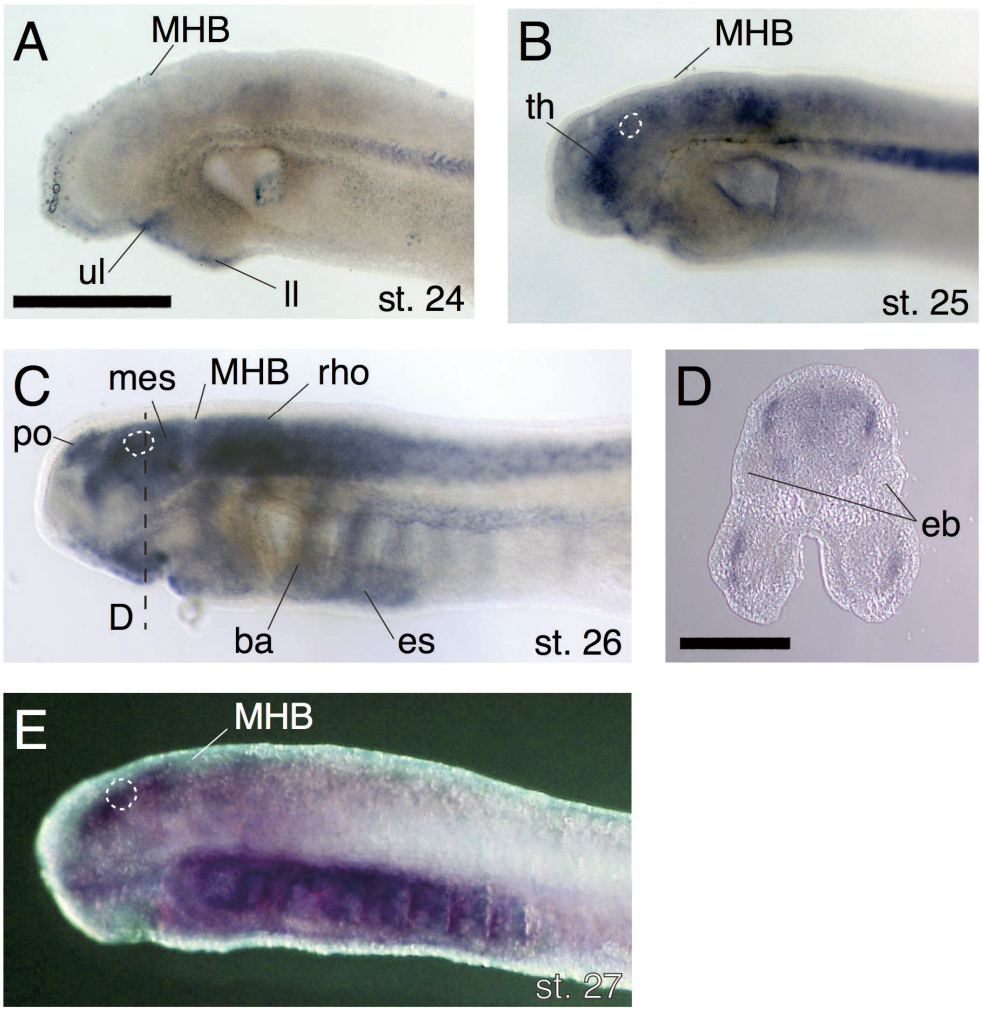
A
MHB
ul
ll
st. 24
B
MHB
th
st. 25
C
mes
MHB
rho
po
D
ba
es
st. 26
D
eb
E
MHB
st. 27

Fig. 2.7. Whole-mount *in situ* hybridization of *EphC* in lamprey embryos and pre-ammocoete larvae (*L. camtschaticum*). White broken lines indicate the presumptive dorsocaudal thalamus and pretectum region, the location of the "primary" optic nerve projecting region. **A:** At stage 23, the craniofacial region. **B:** At stage 24, the whole embryo. At stages **C:** 25 and **D:** 26. **D':** The same specimen as **D** focused on the brain. **E:** Transverse section at the eb level of larvae at stages 26, **F:** 27, and **G:** 28. Abbreviations: ba, branchial arches; eb, eyeball; es, endostyle; fb, forebrain; gV, trigeminal ganglion; gVII, facial ganglion; ll, lower lip; mes, mesencephalon; MHB, mid–hindbrain boundary; os, optic stalk; otv, otic vesicle; rho, rhombencephalon; r3/5/6, rhombomeres 3/5/6, respectively; sm, somites; tel, telencephalon; tg, tegmentum; th, thalamus. Scale bars: 200 μm in **A**, **B**, **C–G** applied in **A** and **B'**.

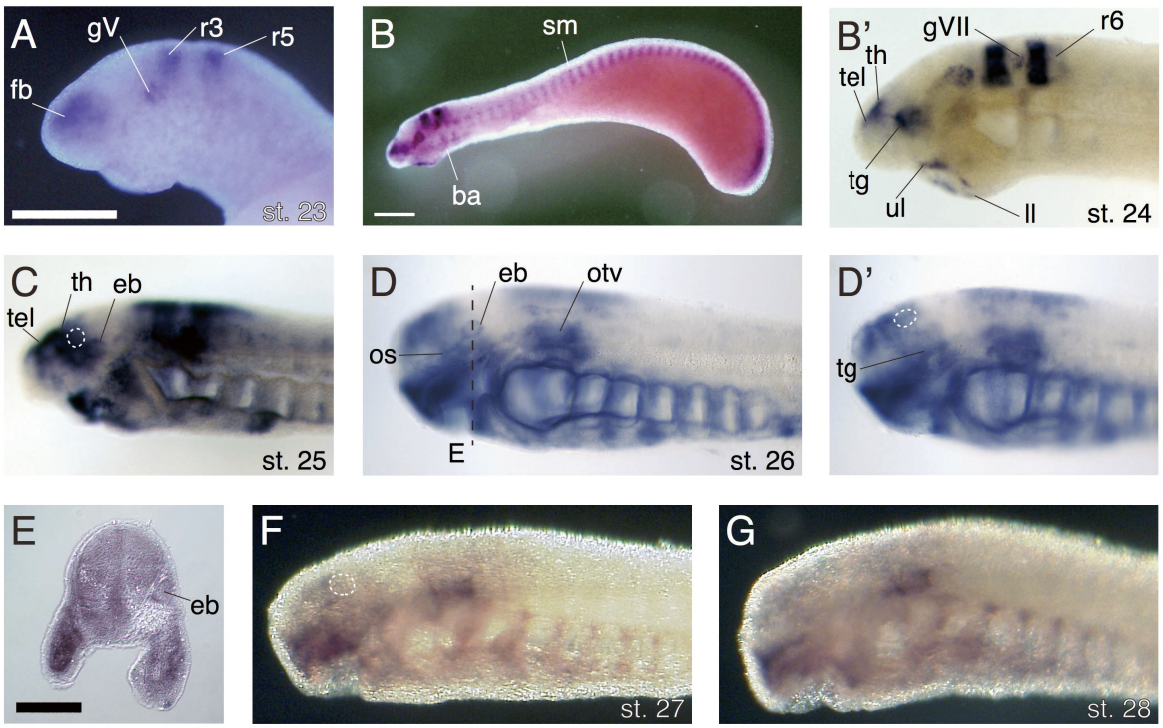
A
gV
r3
r5
fb
st. 23
B
sm
ba
B'
gVII
r6
th
tel
tg
ul
ll
st. 24
C
th
eb
tel
st. 25
D
eb
otv
os
E
st. 26
D'
tg
E
eb
F
st. 27
G
st. 28

Fig. 3.1. Whole-mount immunostaining with anti-acetylated tublin antibody in *L. camtschaticum* embryos and early larvae. Asterisks indicate the eyecup and arrows the optic nerve. **A–D:** Optical microphotographs of specimens stained by DAB in the craniofacial region. **A:** Stage 24. Axonal tracts, including the fasciculus retroflexus, medial longitudinal fascicle, supraoptic tract and the tract of the postoptic commissure. **B:** Stage 25. The tract of the posterior commissure is newly formed. **C:** Stage 25.5. The eyecup (asterisk) and optic nerve (arrow) have appeared. The eyecup region is magnified in the inset. **D:** Stage 26. The eyecup and optic nerve are still distinct. The magnified eyecup region is shown in the inset. **E, F:** Confocal microphotographs of specimens marked by fluorescent secondary antibodies in the head region. **E:** Stage 27. The optic nerve extends to the optic chiasm. The dorsal region of the mesencephalon was less immunoreactive. **F:** Stage 28. The relative position of the eyecup has changed slightly. Abbreviations: Ch, chiasm; FR, fasciculus retroflexus; Mes, mesencephalon; MLF, medial longitudinal fascicle; SOT, supraoptic tract; TPC, tract of the posterior commissure; TPOC, tract of the postoptic commissure. Scale bars: 100 μm.

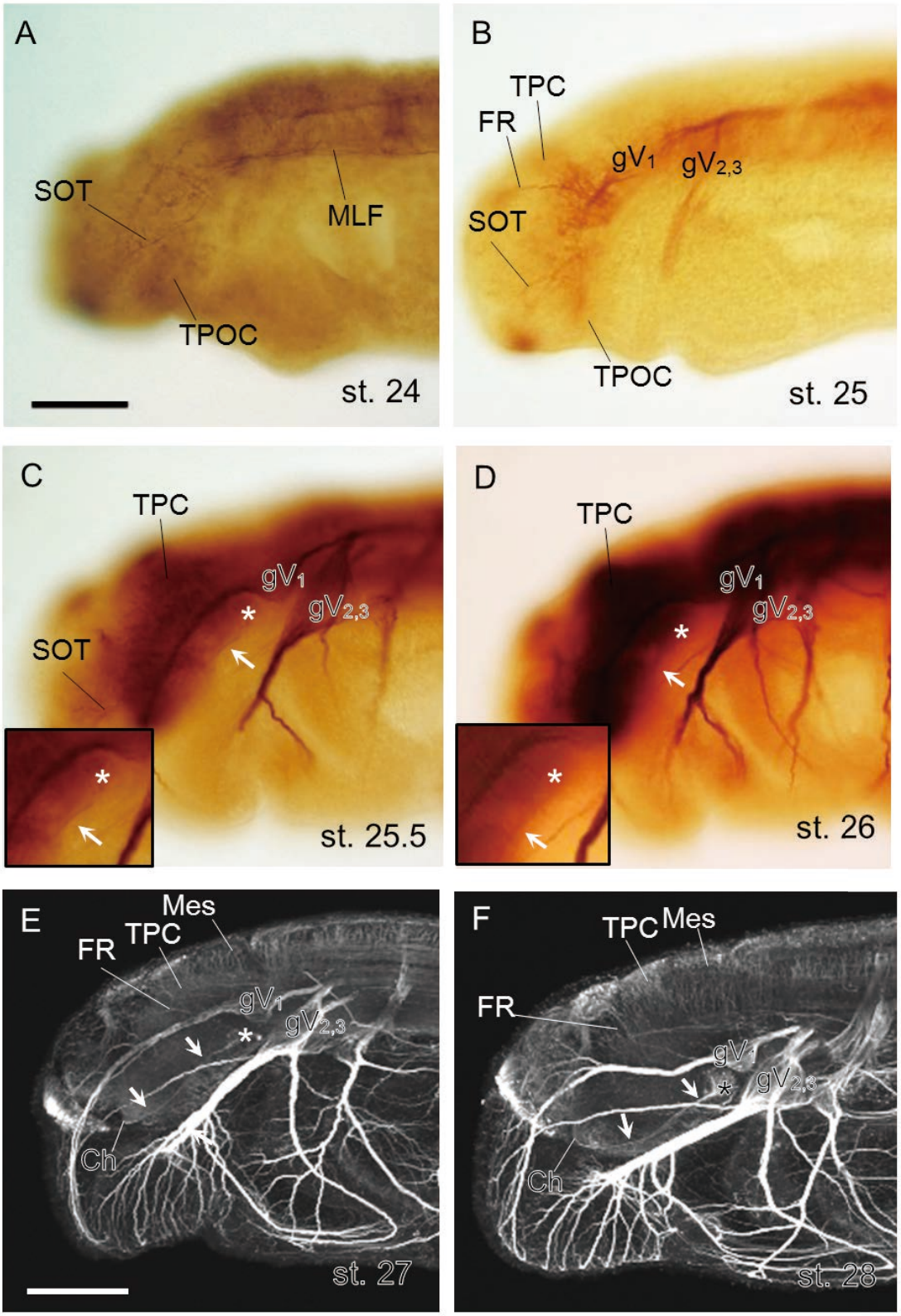
A
SOT
MLF
TPOC
st. 24
B
TPC
FR
gV1
gV2,3
SOT
TPOC
st. 25
C
TPC
gV1
gV2,3
SOT
st. 25.5
D
TPC
gV1
gV2,3
st. 26
E
Mes
TPC
FR
gV1
gV2,3
Ch
st. 27
F
TPC
Mes
FR
gV1
gV2,3
Ch
st. 28

Fig. 3.2. Neurolabeling of lamprey (*L. camtschaticum*) optic nerve fibers. Asterisks indicate the left eyecup. **A:** Overview of the labeled specimen at stage 27. Dextran was injected into the right eyecup (arrowhead), and it travelled through the chiasm, terminating in the left side of the brain. **B–F:** Neurolabeling in serial stages showing target regions. Arrows indicate optic fibers. **B:** Confocal microphotographs of the optic nerve projection region at stage 25.5. Some optic fibers are labeled (arrow). The tract of the posterior commissure is also labeled. **C:** Stage 26. More optic fibers are labeled than at stage 25.5. The tract of posterior commissure is also labeled. **D–F:** Stages 28–30. The number of optic nerves increases but terminates in the same region at all stages (dorsal region of the left eye). Abbreviations: Ch, chiasm; MHB, midbrain-hindbrain boundary; TPC, tract of the posterior commissure. Scale bars: 100 μm.

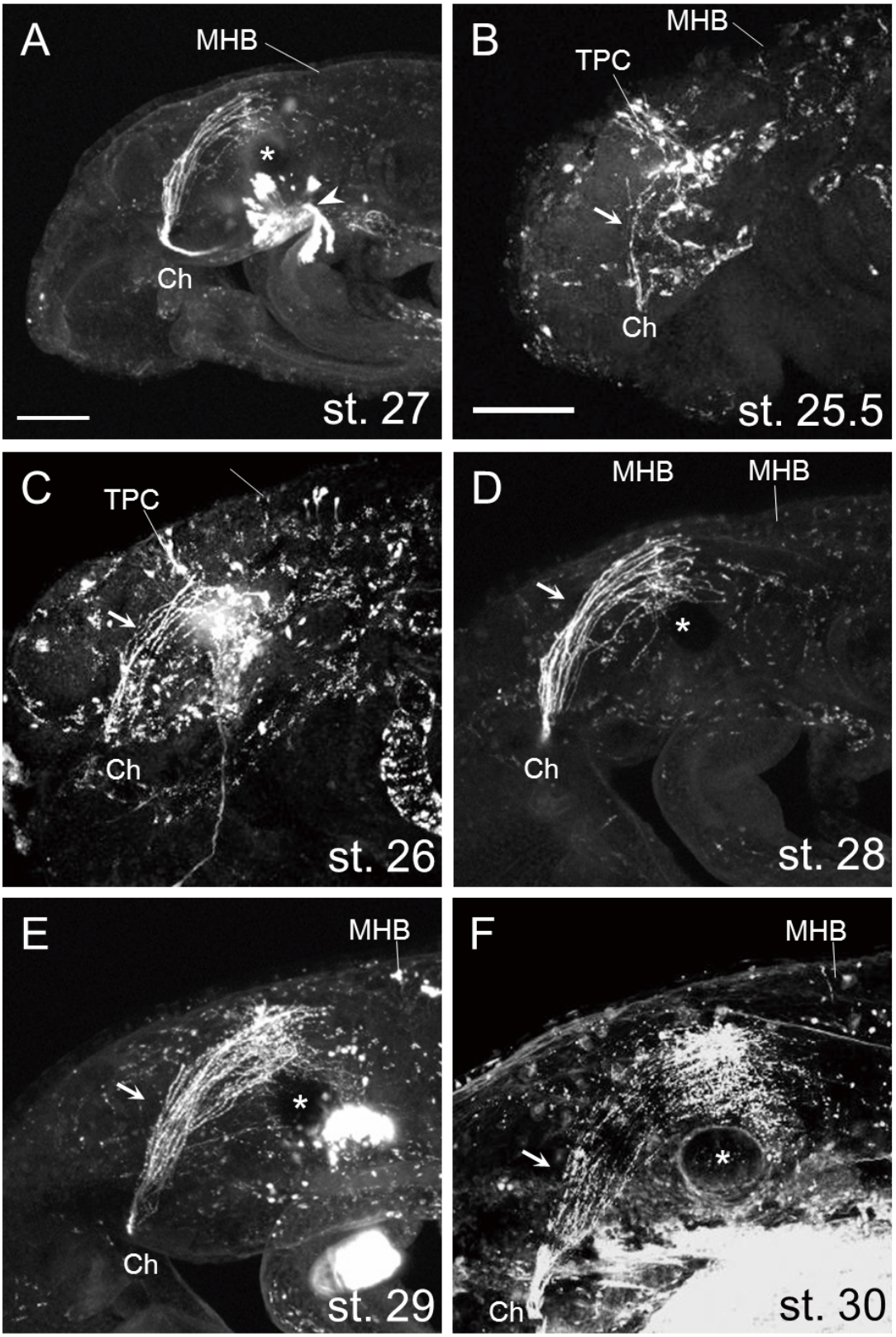
A
MHB
*
Ch
st. 27
B
MHB
TPC
Ch
st. 25.5
C
TPC
Ch
st. 26
D
MHB
MHB
*
Ch
st. 28
E
MHB
*
Ch
st. 29
F
MHB
*
Ch
st. 30

Fig. 3.3 Analysis of the optic nerve projection region in *L. camtschaticum* embryos and early larvae. **A:** Triple labeling of optic fibers, medial longitudinal fascicle and the tract of the posterior commissure in stage 27. **B:** Two-color double labeling of optic fibers (magenta) and medial longitudinal fascicle (green). The optic nerve projects to the dendrites of neurons of the nucleus of the medial longitudinal fascicle neurons. A magnified picture of optic fibers with varicosities (arrowheads) is shown in the inset. This picture was reconstructed from raw data before making the projection picture **B1**. **C:** Double staining of anti-acetylated tubulin antibody immunostaining and *Pax6 in situ* hybridization. **C1** shows anti-acetylated tubulin, **C2** shows *Pax6* expression by transmitted light and **C3** shows the merged microphotographs. The TPC is located in the caudal-most *Pax6*-positive region (arrow), and the nucleus of the medial longitudinal fascicle is located in its ventral region. **D:** Two-color double labeling of optic fibers (magenta) and medial longitudinal fascicle (green) in medaka. **D1** shows dorsal view of the brain region at 10dpf (days post fertilization). **D2** shows magnified left tectal region. Abbreviations: MHB, midbrain-hindbrain boundary; (n)MLF, (nucleus of) medial longitudinal fascicle; TPC, tract of the posterior commissure; tel, telencephalon; ON, optic nerve fibers. Scale bars: 100 μm in **A**, **C1**, **D1**, and **D2**, 50 μm in **B1**.

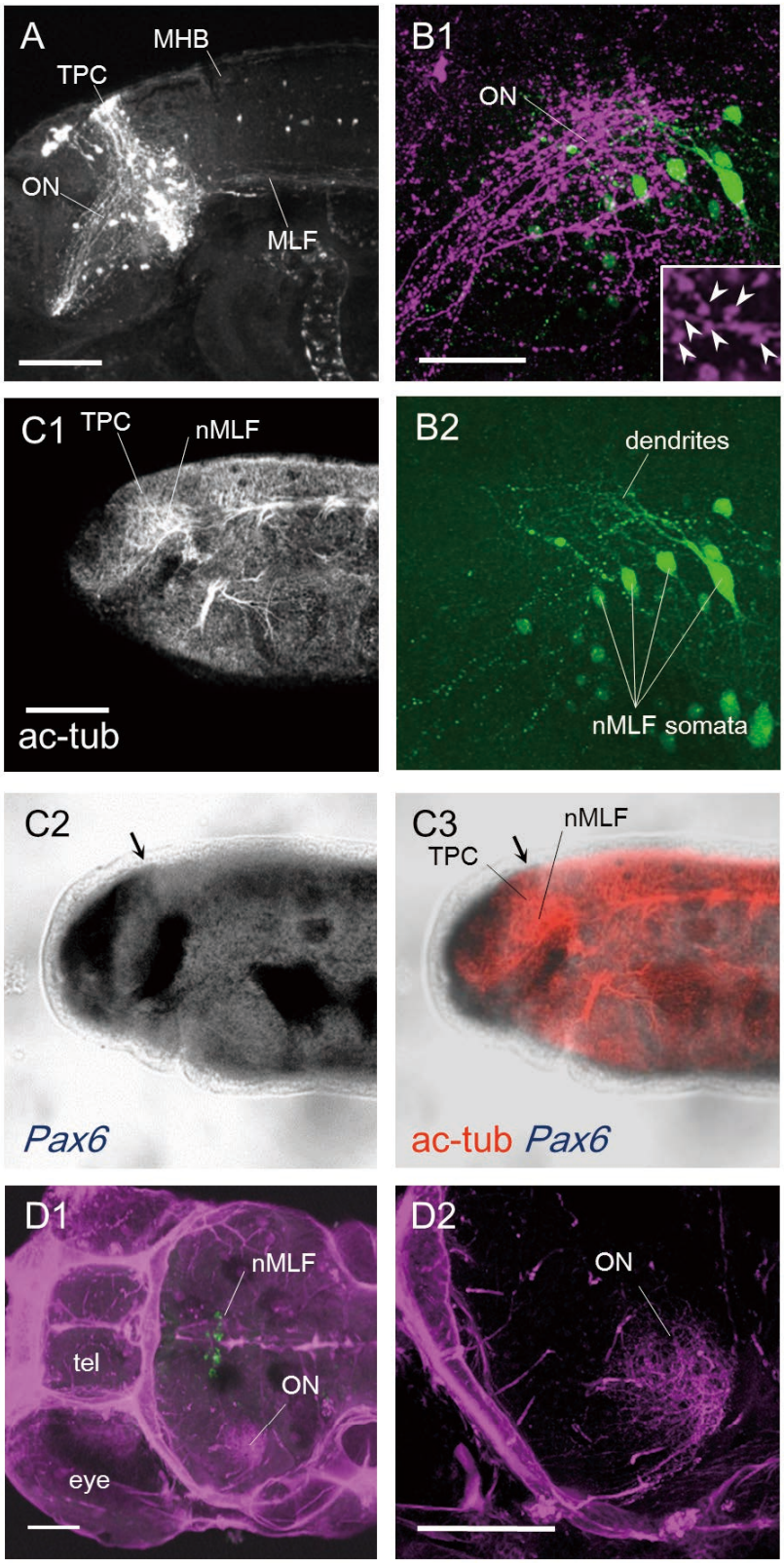
A
MHB
TPC
ON
MLF
B1
ON
C1
TPC
nMLF
ac-tub
B2
dendrites
nMLF somata
C2
Pax6
C3
nMLF
TPC
ac-tub Pax6
D1
nMLF
tel
ON
eye
D2
ON

Fig. 3.4. Neuroarchitecture and brain patterning of amphioxus larvae. **A–C:** Immunohistochemistry in *B*. *lanceolatum* four-gill slit (4gs) larvae. **A:** Immunostaining with anti-serotonin (5-HT) antibody. There are immunoreactive R2 photoreceptor cells just ventral to the frontal eye pigment observed by transmitted light (TR). **B:** Immunostaining with anti-VAChT antibody. Motor neurons in the ventral neural tube were immunoreactive (arrows), and most rostral cells were thought to be giant cells. **C:** Double staining with anti-synaptotagmin (syt, magenta) and anti-acetylated tubulin (ac-tub, green). **C1** shows synaptotagmin immunoreactivity and **C2** shows the merged microphotographs. The presumptive visual center (arrows) is relatively highly anti-synaptotagmin-immunoreactive, and this region is located just rostral to the root of the n2 nerve. **D:** Double staining with anti-acetylated tubulin antibody immunostaining and *Pax6 in situ* hybridization in *B*. *japonicum* one-gill slit (1gs) larvae. **D1** shows *Pax6* expression and **D2** shows the merged microphotographs. The caudal part of the cerebral vesicle is *Pax6*-positive (arrows), and this region corresponds to the presumptive visual center, located just rostral to the root of the n2 nerve. The arrow indicates the second nerve root. **E:** Schematic illustration of the neuroarchitecture and brain patterning of amphioxus larvae. Abbreviations: FEP, frontal eye pigment; GCs: giant cells; (r)N2, (root of) n2 nerve; NP, neuropore; POP, preoral pit; R2Cs, row 2 cells. Scale bars: 50 μm.

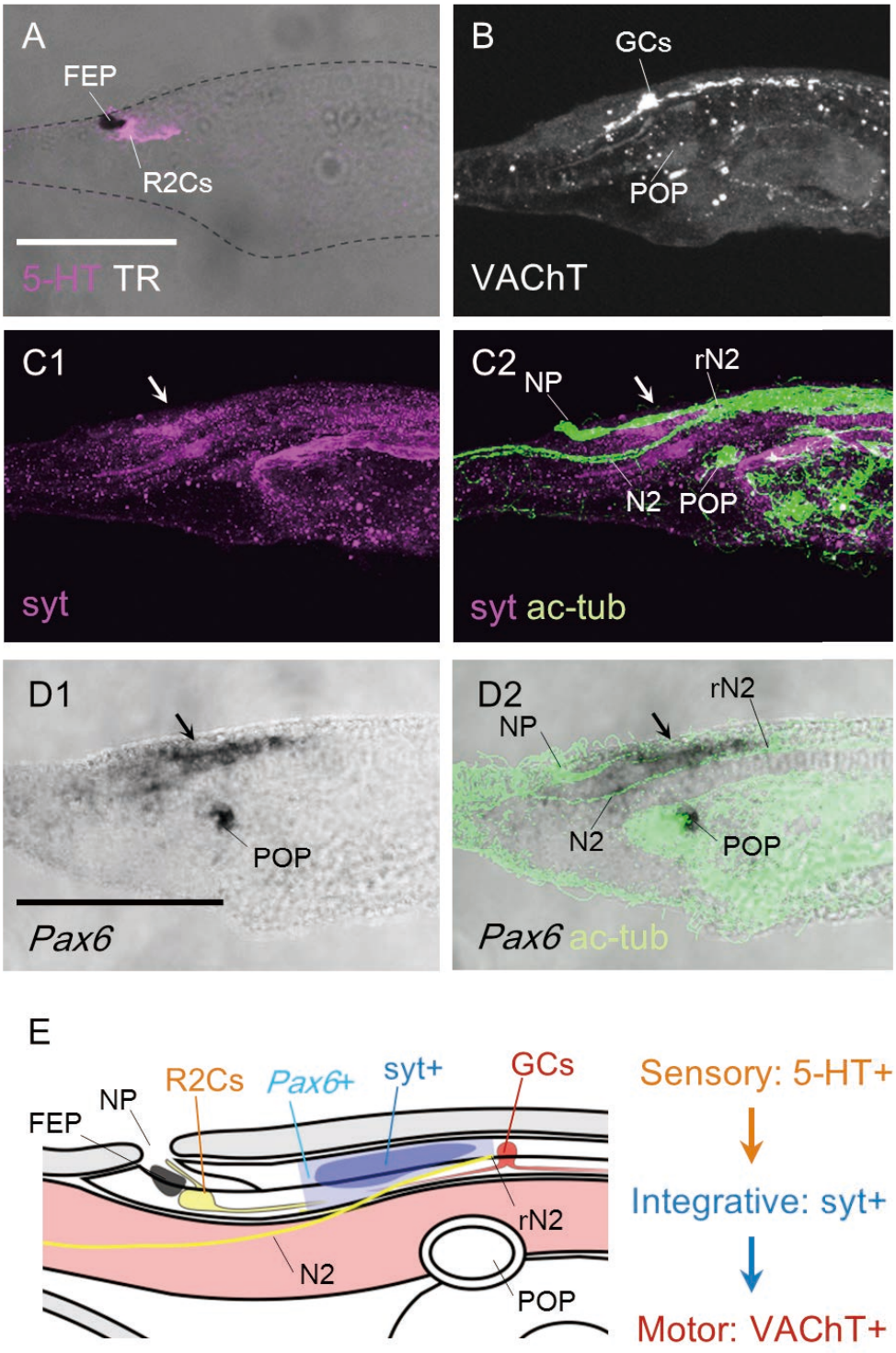
A
FEP
R2Cs
5-HT TR
B
GCs
POP
VAChT
C1
syt
C2
NP
rN2
N2
POP
syt ac-tub
D1
POP
Pax6
D2
NP
rN2
N2
POP
Pax6 ac-tub
E
FEP
NP
R2Cs
Pax6+
syt+
GCs
rN2
N2
POP
Sensory: 5-HT+
Integrative: syt+
Motor: VAChT+

Fig. 3.5. Schematic illustration of the evolution of vertebrate image-forming vision. **A:** Hypothetical evolutionary scenario. The common ancestor of chordates had an ocellus-like eye(s), and the visual center was in the *Pax6*-positive region, which processes directional vision. In the common ancestor of vertebrates, the *Pax6*-positive (i.e. prosencephalic; Pros) visual center remained the main visual center, since larval lampreys had the same type of visual system as protochordates. The mesencephalic (Mes) retino-tectal projection was newly formed as a 'secondary' optic tract. **B:** The gene regulatory network that establishes the mesencephalic region in the vertebrate neural tube. Genes with conserved expression in chordates are underlined (the *Gbx* gene is lost in tunicates and is dashed-underlined). Genes with conserved expression in tunicates and vertebrates are in bold.

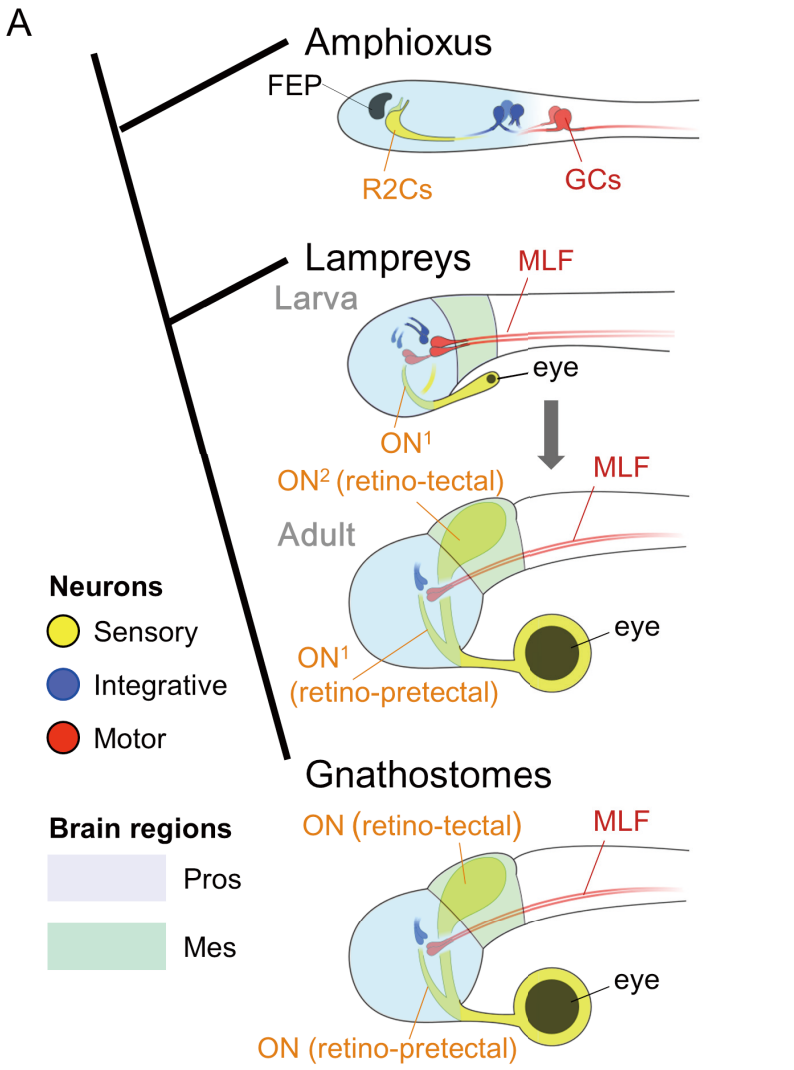
A
Amphioxus
FEP
R2Cs
GCs
Lampreys
Larva
MLF
eye
ON1
ON2 (retino-tectal)
MLF
Adult
eye
ON1
(retino-pretectal)
Neurons
Sensory
Integrative
Motor
Gnathostomes
ON (retino-tectal)
MLF
Brain regions
Pros
Mes
eye
ON (retino-pretectal)
B
Otx2
Gbx2
Fgf8
Wnt1
Pax6
Pax2/5/8
En1/2
ephrinAs
Pros
Mes
ISO

Fig. 4.1. The phylogenetic tree and extra-ocular muscles of the vertebrates. Abbreviations: ao, anterior oblique; ar, anterior rectus; co, caudal oblique; cr, caudal rectus; dr, dorsal rectus; hc, hyoid cavity; hm, hyoid mesoderm; io, inferior oblique; ir, inferior rectus; lr, lateral rectus; m, mouse; mc, mandibular cavity; mm, mandibular mesoderm; mr, medial rectus; ot, otic vesicle; pc, premandibular cavity; pm, premandibular mesoderm; s, somite; vr, ventral rectus; III, oculomotor nerve; IV, trochlear nerve; VI, abducens nerve.

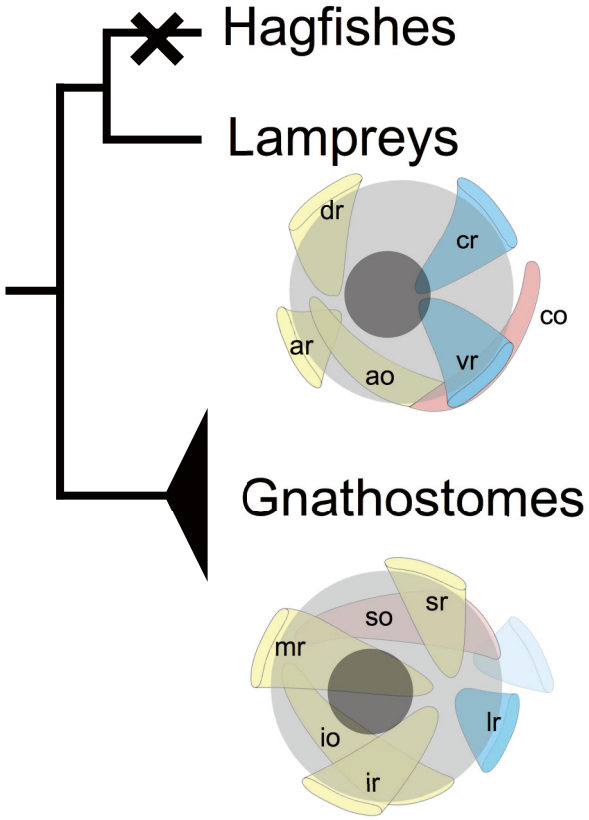
Hagfishes
Lampreys
dr
cr
co
ar
ao
vr
Gnathostomes
sr
so
mr
lr
io
ir

Fig. 4.2. Histological analysis by the hematoxylin-eosin (HE) staining on the extraocular muscles. **A:** Small larva (3.5 cm, about a half year old). **B:** Large larva (10 cm). **C:** Metamorphic lamprey. **D:** Adult lamprey. **A-D1:** External, raw; **A-D2:** External, colored; **A-D3:** Internal, raw; **A-D4:** Internal, colored. Abbreviations: ao, anterior oblique; ar, anterior rectus; co, caudal oblique; cr, caudal rectus; dr, dorsal rectus; vr, ventral rectus. Scale bars: 50 μm in **A1**, 200 μm in **B1**, **C1**, 500 μm in **D1**.

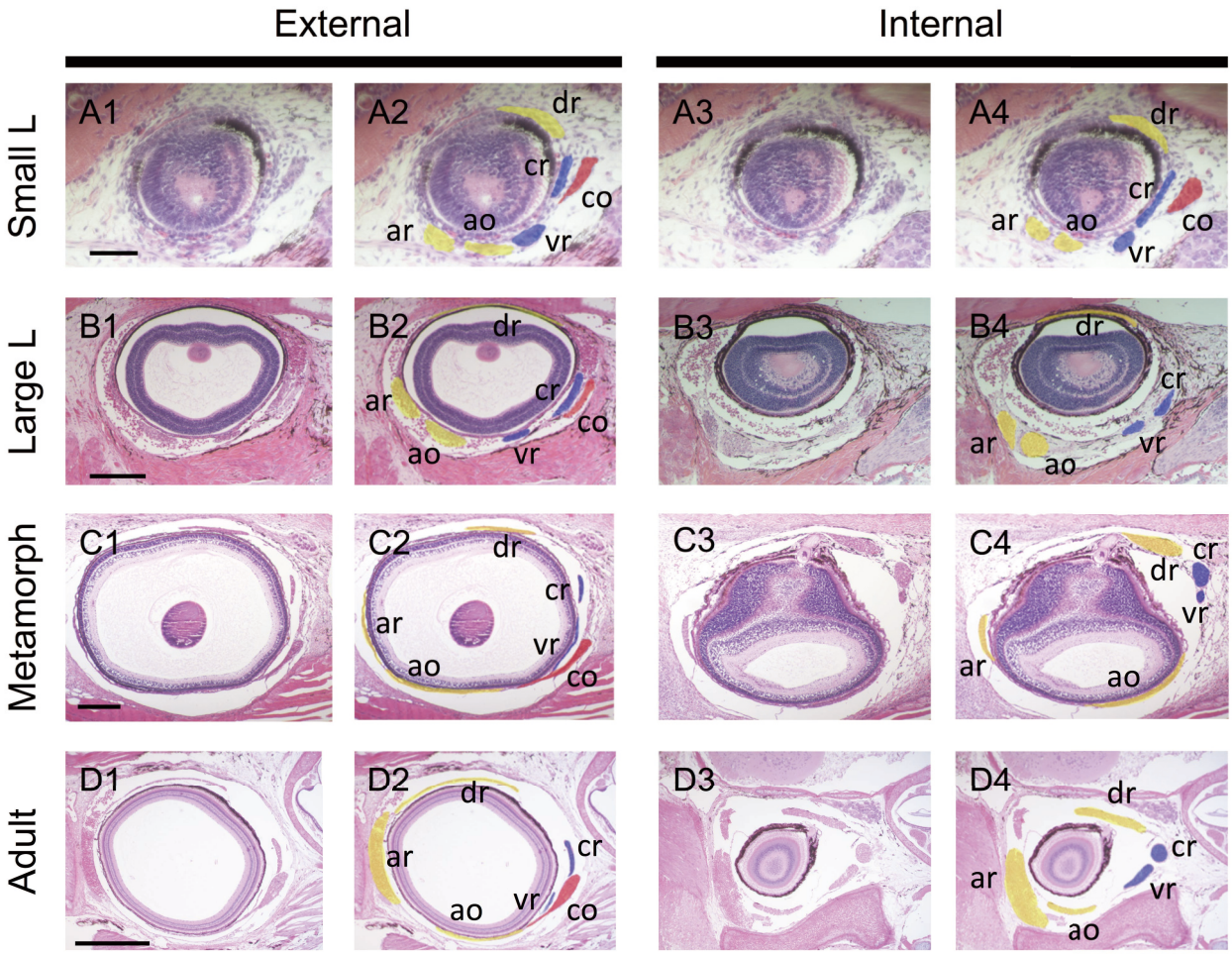
External
Internal
Small L
Large L
Metamorph
Adult
A1
A2
A3
A4
B1
B2
B3
B4
C1
C2
C3
C4
D1
D2
D3
D4
dr
cr
co
ar
ao
vr

Fig. 4.3. Whole-mount immunofluorescence with CH1 (tropomyosin) antibody. **A:** st. 28 prolarva. **B:** st. 30 prolarva (**B1:** Overview; **B2:** Internal). **C:** 32mm larva (**C1:** Raw; **C2:** Colored). Abbreviations: ao, anterior oblique; ar, anterior rectus; cb, constrictor buccalis; co, caudal oblique; cr, caudal rectus; dr, dorsal rectus; elv, elevator labialis ventralis; suboc, subocuralis; supraoc, supraoclularis; vc, velocranialis; vr, ventral rectus. Scale bar: 100 μm.

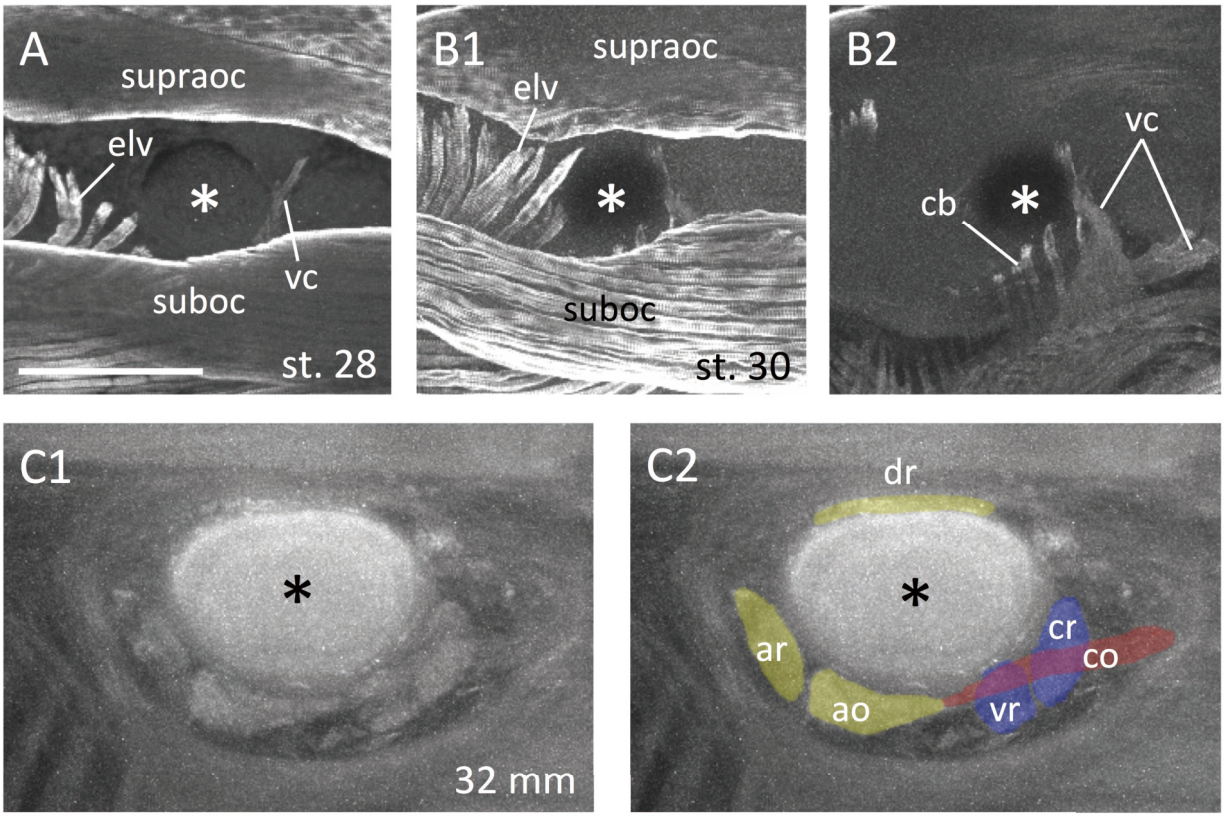
A
supraoc
elv
*
vc
suboc
st. 28
B1
supraoc
elv
*
suboc
st. 30
B2
vc
cb
*
C1
*
32 mm
C2
dr
*
ar
cr
co
ao
vr

Fig. 4.4. Whole-mount *in situ* hybridization in st. 26 lamprey prolarvae. **A:** *PitxA* (**A1:** Lateral view; **A2, 3:** Sections). **B:** *Gsc* (**B1:** Lateral view; **B2:** Section). **C:** *TbxA* (**C1:** Lateral view; **C2:** Section). **D:** Schematic illustration of the *PitxA*, *Gsc*, and *TbxA* expression patterns. Abbreviations: hm, hyoid mesoderm; ll, lower lip; m, mouse; mm, mandibular mesoderm; oe, oral epithelium; ot, otic vesicle; pm, premandibular mesoderm; pp; phalangeal pouch, s, somite; vl, velum; vr, ventral rectus. Scale bar: 200 μm.

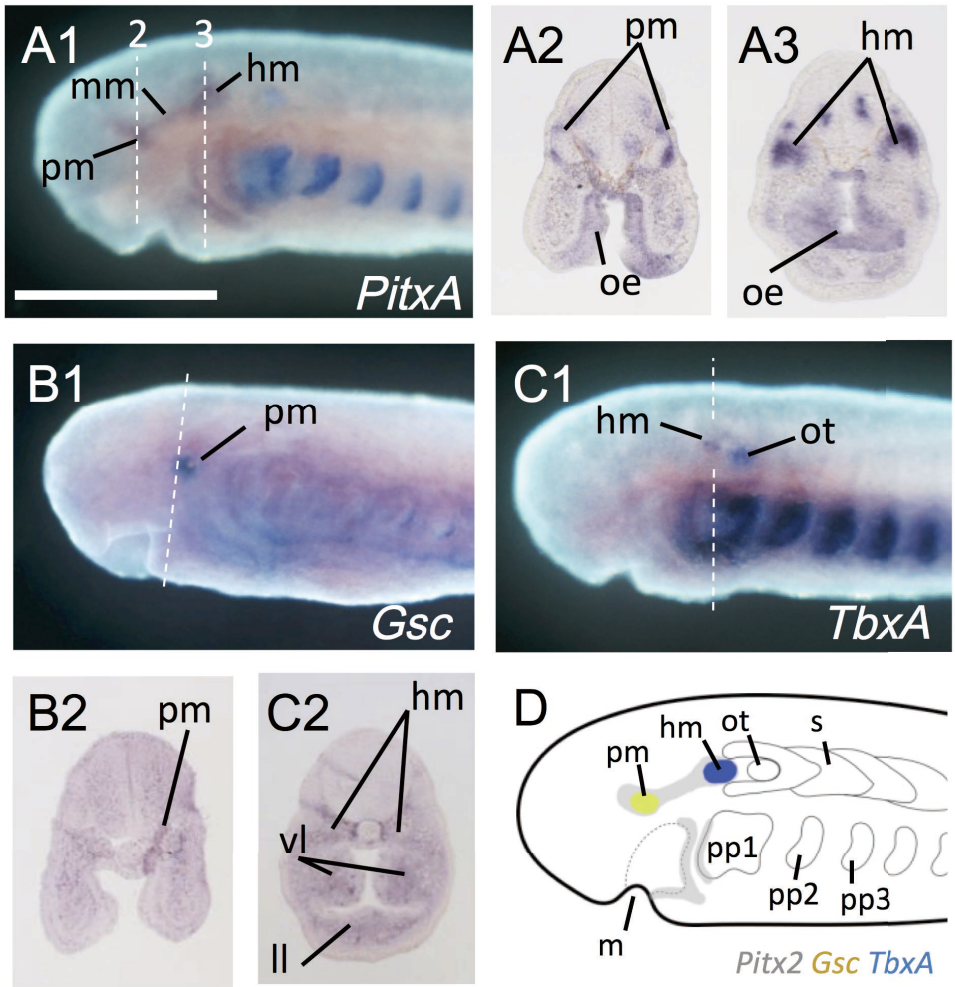
A1
2
3
mm
hm
pm
PitxA
A2
pm
oe
A3
hm
oe
B1
pm
Gsc
C1
hm
ot
TbxA
B2
pm
C2
hm
vl
ll
D
hm
ot
s
pm
pp1
pp2
pp3
m
Pitx2 Gsc TbxA

Fig. 4.5. Sections *in situ* hybridization in 9cm ammocoete larvae. **A:** *PitxA* . **B:** *MrfA*. **C:** *MA2*.

Arrows; the expression in the EOMs. Scale bar: 200 μm.

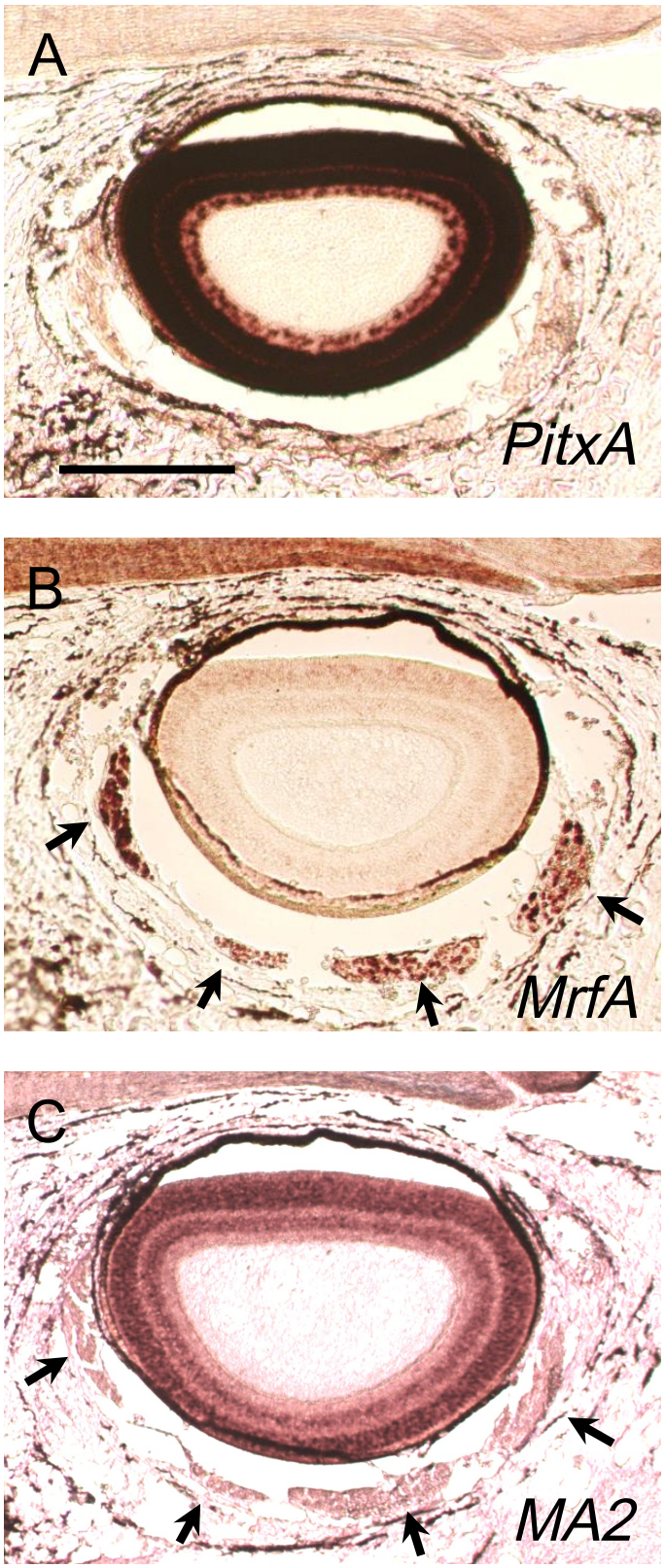
A
PitxA
B
MrfA
C
MA2

Fig. 4.6. Nerves innervating head mesoderm subpopulations and EOMs. **A:** *PitxA* expression in st. 28. **B:** Double staining of *PitxA in situ* hybridization (bright field) and acetylated tubulin antibody immunofluorescence (red). **C-D:** Single immunofluorescence with acetylated tubulin antibody. **C:** st. 28 (**C1:** Overview; **C2:** magnified dashed box region in **C1**). **C:** 15mm larva. **D:** 35mm larva. Abbreviations: gV_1, ophthalmicus profundus nerve ganglion; $gV_{2,3}$, maxillomandibular nerve ganglion; gVII, facial nerve ganglion; mm, mandibular mesoderm; ot, otic vesicley; pm, premandibular mesoderm; II, optic nerve; III, oculomotor nerve; IV, trochlear nerve; VI, abducens nerve. Scale bars: 200μm in **A**, 100 μm in **D**, **E**.

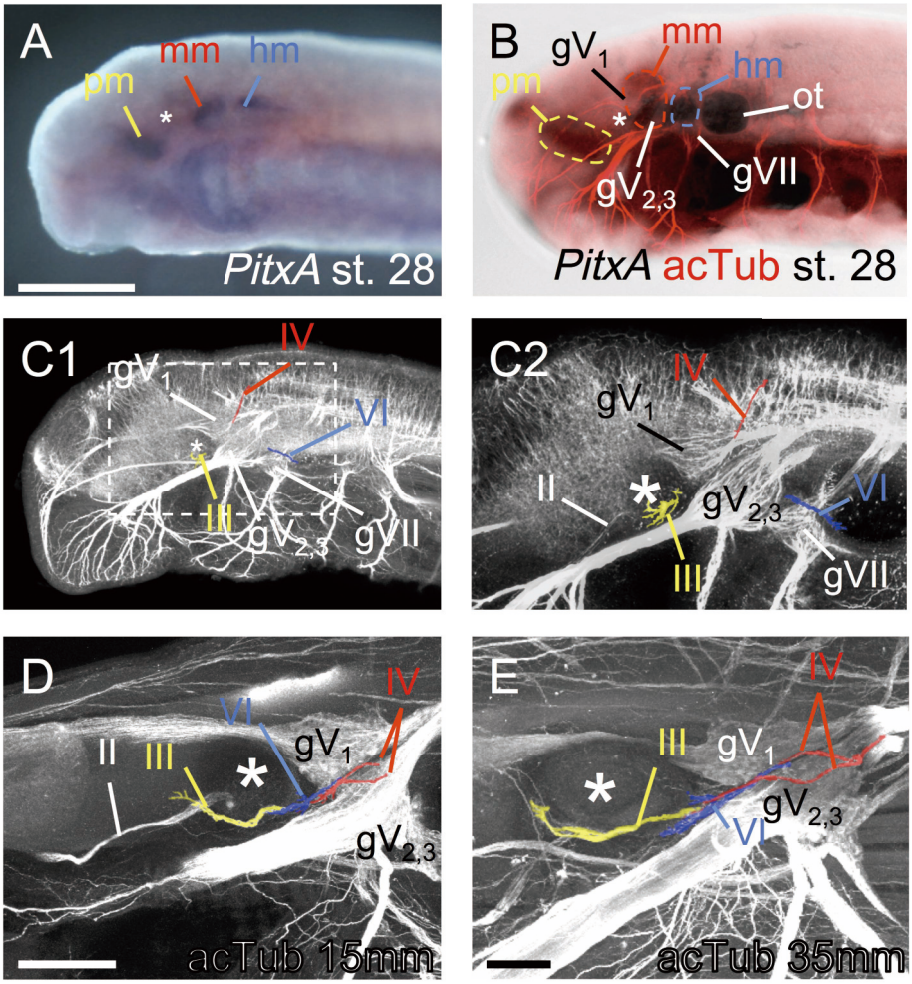
A
mm
hm
pm
*
PitxA st. 28
B
gV1
mm
hm
pm
ot
*
gVII
gV2,3
PitxA acTub st. 28
C1
gV1
IV
VI
*
III
gV2,3
gVII
C2
IV
gV1
II
*
gV2,3
VI
III
gVII
D
VI
IV
II
III
*
gV1
gV2,3
acTub 15mm
E
IV
III
gV1
*
gV2,3
VI
acTub 35mm

Fig. 4.7. Dye injections on the head mesoderm. **A:** DiO injection into the premandibular mesoderm of the st. 21 embryo. **B:** DiO injected sample in st. 27 (**B1:** DiO fluorescence; **B2:** DiO fluorescence and bright field). DiO fluorescence is observed in the periocular region. **C:** Section in the dashed line plane in **B1** (**C1:** DiO fluorescence; **C2:** DAPI fluorescence). **D:** Three color dye injections on the three mesodermal subpopulations (premandibular; DiO, mandibular; DiI, hyoid; DiD, respectively). **E:** Dye injected sample in st. 27. Three mesodermal subpopulations retained their cohesion. Scale bars: 200μm in **A**, 400 μm in **D**.

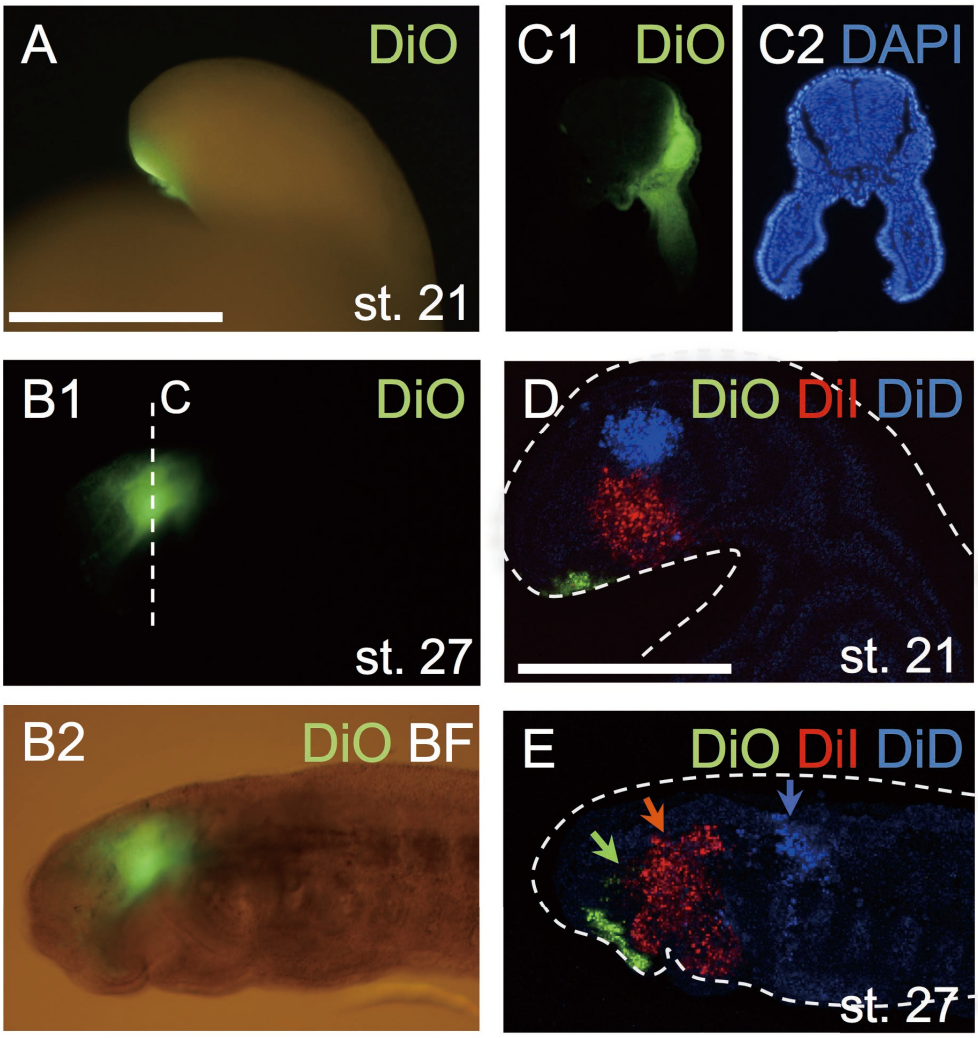
A
DiO
st. 21
C1
DiO
C2
DAPI
B1
C
DiO
st. 27
D
DiO DiI DiD
st. 21
B2
DiO BF
E
DiO DiI DiD
st. 27

Fig. 4.8. Schematic illustration of the comparison of the EOMs development between the lamprey (**A-C**) and shark **(D-F**). **A, D:** Pharyngeal stage. **B, E:** Three head mesodermal subpopulations innervated by respective motor nerves. **C, F:** Differentiated state. Abbreviations: ao, anterior oblique; ar, anterior rectus; co, caudal oblique; cr, caudal rectus; dr, dorsal rectus; hc, hyoid cavity; hm, hyoid mesoderm; io, inferior oblique; ir, inferior rectus; lr, lateral rectus; m, mouse; mc, mandibular cavity; mm, mandibular mesoderm; mr, medial rectus; pc, premandibular cavity; pm, premandibular mesoderm; vr, ventral rectus; III, oculomotor nerve; IV, trochlear nerve; VI, abducens nerve.

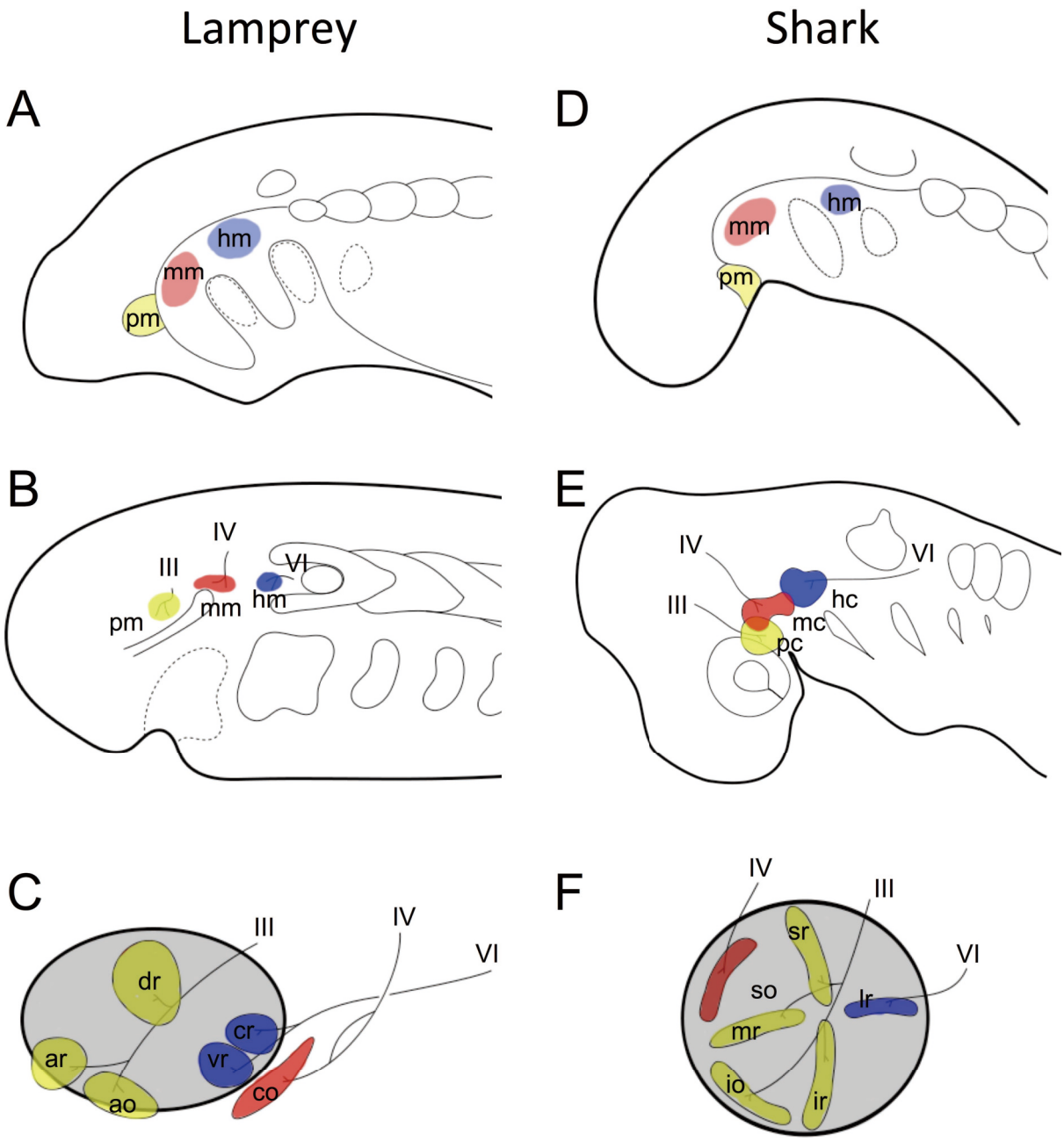
Lamprey
Shark
A
hm
mm
pm
D
hm
mm
pm
B
IV
III
VI
pm
mm
hm
E
IV
VI
III
hc
mc
pc
C
III
IV
VI
dr
cr
ar
vr
co
ao
F
IV
III
sr
VI
so
lr
mr
io
ir

Fig. 4.9. Hypothetical scenario for the evolution of the EOMs. In the common ancestor of the vertebrates had unsegmented head mesoderm but there were three subpopulations with distinct genetic patterning and motor nerve innervation. They had lamprey-type EOMs and it was conserved in Osteostracans and Placoderms (in hagfishes, EOMs are completely degenerated). In the common ancestor of the crown gnathostomes, the disposition of the EOMs was changed to extant-gnathostomes-type.

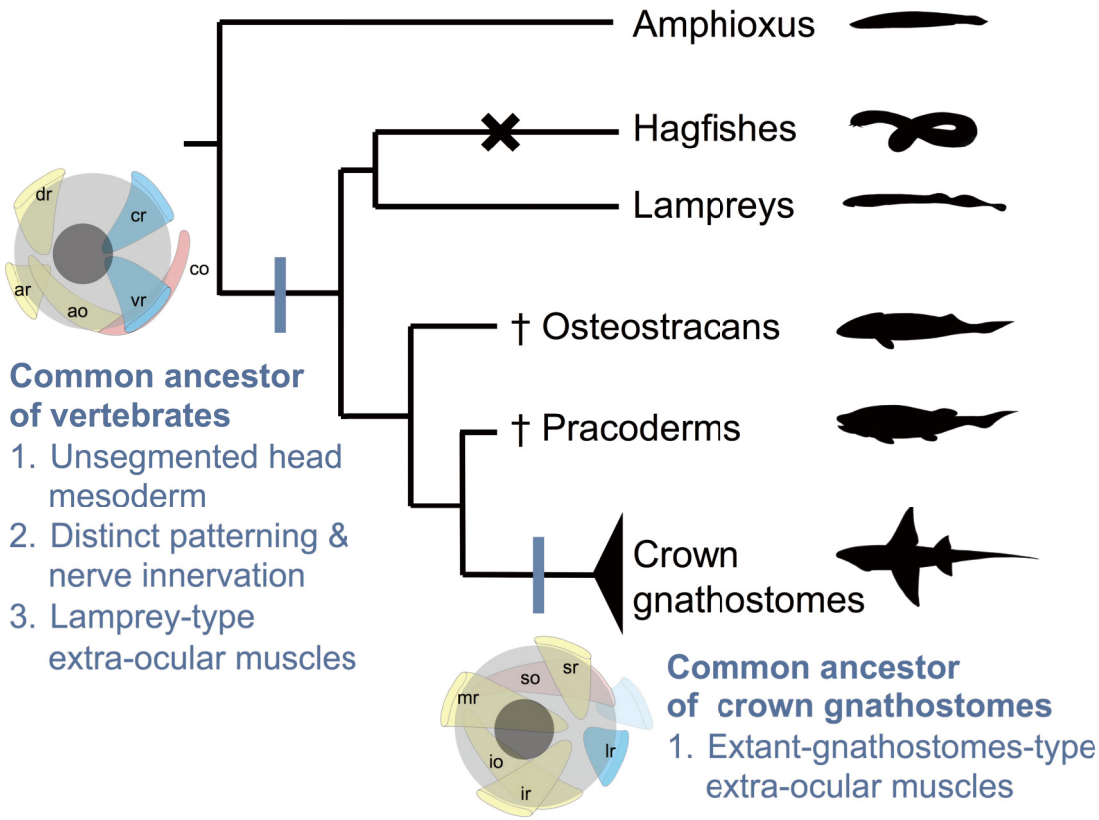
Amphioxus
Hagfishes
Lampreys
† Osteostracans
† Pracoderms
Crown gnathostomes
dr
cr
co
ar
ao
vr
Common ancestor of vertebrates
1. Unsegmented head mesoderm
2. Distinct patterning & nerve innervation
3. Lamprey-type extra-ocular muscles
so
sr
mr
lr
io
ir
Common ancestor of crown gnathostomes
1. Extant-gnathostomes-type extra-ocular muscles